ÇUKUROVA UNIVERSITY
INSTITUTE OF NATURAL AND APPLIED SCIENCES

M.Sc. THESIS

Ahmet KAPLAN

THERMODYNAMIC AND EXERGOECONOMIC ANALYSIS OF TWO-STAGE ORGANIC RANKINE CYCLE USING DIFFERENT REFRIGERANTS

DEPARTMENT OF MECHANICAL ENGINEERING

ADANA-2022

ÇUKUROVA UNIVERSITY
INSTITUTE OF NATURAL AND APPLIED SCIENCE

THERMODYNAMIC AND EXERGOECONOMIC ANALYSIS OF TWO STAGE ORGANIC RANKINE CYCLE USING DIFFERENT REFRIGERANTS

Ahmet KAPLAN

MSc THESIS

DEPARTMENT OF MECHANICAL ENGINEERING

We certify that the thesis titled above was reviewed and approved for the award of the degree of the Master of Science by the board of jury on 28 / 01 /2022.

………………………………..	………..……………….........	……………………………………
Assoc.Prof.Dr. Arif ÖZBEK	Assoc.Prof.Dr.Fırat EKİNCİ	Assoc.Prof.Dr.GöktürkM.ÖZKAN
SUPERVISOR	MEMBER	MEMBER

This MSc thesis is written at the Department of Mechanical Engineering, Institute of Natural and Applied Sciences of Çukurova University.
Registration Number:

Prof. Dr. Sadık DİNÇER
Director
Institute of Natural and Applied Sciences

ABSTRACT

MSc. THESIS

THERMODYNAMIC AND EXERGOECONOMIC ANALYSIS OF TWO-STAGE ORGANIC RANKINE CYCLE USING DIFFERENT REFRIGERANTS

Ahmet KAPLAN

ÇUKUROVA UNIVERSITY
INSTITUTE OF NATURAL AND APPLIED SCIENCES
DEPARTMENT OF MECHANICAL ENGINEERING

Supervisor : Asoc.Prof.Dr. Arif ÖZBEK
Year: 2022, Pages: 51
Jury : Assoc.Prof.Dr. Arif ÖZBEK
: Assoc.Prof.Dr. Fırat EKİNCİ
: Assoc.Prof.Dr. Göktürk M. ÖZKAN

In this study, A two-stage Organic Rankine Cycle (ORC) was analyzed by using engineering equation solver (EES). Twelve Organic working fluids used in R32, R227ea, R410a, R290, R134a, RC318, R407c, R22, R23, R116, R218 and R245fa are used as the working fluids for given temperature limits. Suitable choice of refrigerant or refrigerant couple for the ORC's cycle efficiency, exergy and net work output has a vital importance. The results showed that the highest net power output and the highest thermal efficiency were obtained from the R23 + R23 pair at 425K. R227ea + R410a couple gives the highest thermal efficiency at 355K. For R245fa + R245fa refrigerant at 425K, 14.11kW exergy destruction is obtained in Pump-1, higher than other components. The smallest exergy destruction of 0.133kW is observed in Turbine-2 at 400K temperature. As a result, this study showed us R245fa is the most suitable working fluid because of higher condensation temperature for environmental conditions.

Key Words: Organic Rankine Cycle, Two Stage Process, Solar Power

ÖZ

YÜKSEK LİSANS TEZİ

FARKLI SOĞUTUCU AKIŞKANLAR KULLANILARAK İKİ AŞAMALI ORGANİK RANKİNE ÇEVRİMİNİN TERMODİNAMİK VE EKSERGOEKONOMİK ANALİZİ

AHMET KAPLAN

ÇUKUROVA ÜNİVERSİTESİ
FEN BİLİMLERİ ENSTİTÜSÜ
MAKİNE MÜHENDİSLİĞİ ANABİLİM DALI

Danışman : Doç.Dr. Arif ÖZBEK
Yıl: 2022, Sayfa: 51
Jüri : Doç.Dr. Arif ÖZBEK
: Doç.Dr. Fırat EKİNCİ
: Doç.Dr.Göktürk M.ÖZKAN

Bu çalışmada, iki aşamalı bir Organik Rankine Döngüsü (ORC), mühendislik denklem çözücüsü (EES) kullanılarak analiz edilmiştir. R32, R227ea, R410a, R290, R134a, RC318, R407c, R22, R23, R116, R218 ve R245fa'da kullanılan on iki Organik çalışma sıvısı, verilen sıcaklık limitleri için çalışma sıvısı olarak kullanılmıştır. ORC'nin çevrim verimliliği, ekserjisi ve net iş çıkışı için uygun soğutucu veya soğutucu çifti seçimi hayati bir önem taşımaktadır. Sonuçlar, en yüksek net güç çıkışının ve en yüksek ısıl verimliliğin 425K'da R23 + R23 çiftinden elde edildiğini göstermektedir. R227ea + R410a çifti, 355K'da en yüksek ısıl verimliliği sağlamıştır. 425K'da R245fa + R245fa soğutucu akışkan için Pompa-1'de diğer bileşenlerden daha yüksek 14.11kW ekserji tahribatı elde edilmiştir. 0.133kW'lık en küçük ekserji yıkımı, 400K sıcaklıkta Türbin-2'de gözlenmektedir. Sonuç olarak, bu çalışma bize R245fa'nın çevresel koşullar için daha yüksek yoğuşma sıcaklığı nedeniyle en uygun çalışma sıvısı olduğunu göstermiştir.

Anahtar Kelimeler: Organik Rankine Çevrimi, Çift Kademeli İşlem, Güneş Enerjisi

EXPANDED ABSTRACT

Nowadays energy is the most important thing for our world. And people is searching the alternative way to generate the energy. Basic principles of ORC, very similar to the conventional Rankine cycle. However, the main difference is the use of organic working fluid of the ORC. Studies shows the output power and efficiency of two-stage ORC system are 38.9% higher than that of single-stage system. Low heat sources can be converted to electrical energy and these can be used in an ORC system design.

The Organic Rankine Cycle (ORC) is use of an organic fluid occurring at a lower temperature than the water-steam phase change. The organic fluid allows Rankine cycle heat recovery from lower temperature sources such as solar power, industrial waste heat, geothermal heat, etc. The low temperature heat is produce useful work that can itself be converted into electricity. This system consists of two stages. In the first and second stages, the same fluid is used and the heat taken from the solar collector is converted into electrical energy. Solar collector can be change with all of the heat sources. The system operates with a constant mass flow rate and pressure in the first and second stages. In this work, the Organic Rankine Cycle, which provides economic electricity generation when used in renewable energy power plants operating at low temperatures and having a limited output power. Energy analysis of a double-stage Organic Rankine Cycle (ORC) was performed using the Engineering Equation Solver program (EES). Firstly, Five Organic working fluids used in this study are in the second stage R410a constant and the first stage R32, R227ea, R410a, R290 and R134a are used as the working fluids for a given temperature limits. The purpose of this work is to determine the effect of working fluid to system efficiency and find out the best suitable working fluid couple. Secondly, In the first and second stages, eight different organic working fluids (R134a, R410a, RC318, R407c, R22, R23, R116, and R218) were used in pairs for certain temperature limits. Choosing a suitable refrigerant or refrigerant

pair is crucial for the ORC's high thermal efficiency and net work output value. This study aims to determine the effect of working fluid on system efficiency and find out the most suitable working fluid pair. Lastly, R245fa is used as a refrigerant in the first and second stages for certain temperature limits. The purpose of work is determine the effect of working temperature on system efficieny, exergy efficiency and find out the most suitable working temperature.

The results first work showed that R227ea + R410a couple gives the highest thermal efficiency but highest net power output is obtained R290 + R410a refrigerant couples. R410a is constant for second stage and R134a, R32, R410a, R290, R227ea is changed for first stage. It is clearly seen that thermal efficiency R227ea + R410a, R290 + R410a and R134a + R410a couples decreases when the temperature is increased. Furthermore, R290 + R410a couple gave the %28.9 higher net power output then R32 + R410a couple. And R227ea + R410a couple gave the smallest net power output. R32 + R410a couple gives %41 more power output then R134a + R410a couple. The second calculation showed that the highest net power output and the highest thermal efficiency were obtained from the R23 + R23 pair. When the R23 + R23 pair is used and turbine inlet temperature is 425 K in the ORC system, the thermal efficiency is 4.31% greater than the R22 + R22 pair. The system's thermal efficiency increases with temperature when R23 + R23, R22 + R22, R410a + R410a and R407c + R407c refrigerant pairs use. Among all refrigerants, R23 can be recommended for all working temperatures. Because R23 + R23 pair gives the highest net power output and thermal efficiency values for all temperatures and working fluids. The thermal efficiency of other pairs decreases when the temperature is increased. On the other hand, when R218 + R218 pair is used, the smallest system thermal efficiency value among the other pairs was obtained at all temperatures. It was also observed that the lowest net power output from the RC318 + RC318 pair, increasing the turbine's inlet temperature has a negative impact on the thermal efficiency of the RC318 + RC318 pair. That thermal efficiency dramatically decreases from 6.708 to 5.338. It is observed that the thermal efficiency of R22, R407c, R410a and R23 increases as the temperature increases. On the other hand, in other refrigerants, the thermal efficiencies decreased as the temperature increased, and the lowest thermal efficiency was obtained from the R218 + R218 pair. The exergy efficiency of the cycle decreases with increasing evaporator inlet temperature. At same time, thermal efficiency of the system decreases with increasing evaporator inlet temperature. The highest thermal and exergy efficiencies are seen at the 400K temperature. exergy efficiency and exergy destruction values versus evaporator inlet temperature for Turbine1 and 2. It is seen from the figure that, exergy efficiency in the Turbine-1 decreases, while exergy destruction in the Turbine-1 increases with increasing evaporator inlet temperature. The smallest and highest exergy destructions in the Turbine-1 is 0.4514 kW and 0.6653 kW, respectively. The percentage of the exergy efficiency in Turbine-1 is 98.14 and 97.54 for 400K and 425K, respectively. Exergy efficiency in the Turbine-2 decreases, while exergy destruction in the turbine-2 increases, when evaporator inlet temperature is increased. The smallest and highest exergy destruction in the Turbine-2 is 0.1258 kW and 0.1496 kW, respectively. The percentage of the exergy efficiency in Turbine-2 is 99.25 and 98.48 for 400K and 425K, respectively. the exergy efficiency reduces with increasing evaporator inlet temperature of hot fluid for Pump1 and 2. In addition, the highest exergy efficiency is calculated as to be 6.18% and 83% for Pump-1 and 2, respectively when the evaporator inlet temperature is 400K. Exergy efficiency values decrease up to 5.48% and 44% for Pump 1and 2. The greatest efficiencies were obtained in Turbine1 and 2 and in the Evaporator. Smallest efficiencies were obtained in both Condensers and in Pump1. The maximum exergy destruction is found in Pump1 compared to other components for all temperatures. Minimum exergy destruction is found in Turbine2 compared to other components for all temperatures. condenser 1 and 2 outlet temperature values for different refrigerants which is working at 405K. R23 + R23 couples gives smallest condenser 1 and 2 output temperatures which is 218.7K and 190.9K respectively. At the same working condition R245fa

+ R245fa couples givest highest condenser 1 and 2 output temperatures which is 328K and 288K respectively. That means Accourding to ORC which is working at the atmosphere condition is R245fa + R245fa couples suitable because of that couples givest highest condenser 1 and 2 output temperatures which is 328K and 288K respectively.

GENİŞLETİLMİŞ ÖZET

Günümüzde enerji dünyamız için en önemli şeydir. Ve insanlar enerjiyi üretmenin alternatif yolunu arıyorlar. ORC'nin temel ilkeleri, geleneksel Rankine döngüsüne çok benzer. Ancak asıl fark, ORC'nin organik çalışma sıvısının kullanılmasıdır. Çalışmalar, iki kademeli ORC sisteminin çıkış gücünün ve verimliliğinin, tek kademeli sisteme göre %38,9 daha yüksek olduğunu göstermektedir. Düşük ısı kaynakları elektrik enerjisine dönüştürülebilir ve bunlar bir ORC sistem tasarımında kullanılabilir.

Organik Rankine Döngüsü (ORC), su-buhar faz değişiminden daha düşük bir sıcaklıkta meydana gelen bir organik sıvının kullanılmasıdır. Organik sıvı, güneş enerjisi, endüstriyel atık ısı, jeotermal ısı vb. gibi daha düşük sıcaklık kaynaklarından Rankine çevrimi ısı geri kazanımına izin verir. Düşük sıcaklıktaki ısı, kendisi elektriğe dönüştürülebilen faydalı işler üretir. Bu sistem iki aşamadan oluşmaktadır. Birinci ve ikinci aşamalarda aynı akışkan kullanılır ve güneş kollektöründen alınan ısı elektrik enerjisine dönüştürülür. Güneş kollektörü tüm ısı kaynakları ile değiştirilebilir. Sistem, birinci ve ikinci kademelerde sabit kütlesel debi ve basınçla çalışır. Bu çalışmada, düşük sıcaklıklarda çalışan ve sınırlı çıkış gücüne sahip yenilenebilir enerji santrallerinde kullanıldığında ekonomik elektrik üretimi sağlayan Organik Rankine Çevrimi ele alınmıştır. Çift aşamalı Organik Rankine Döngüsünün (ORC) enerji analizi, Engineering Equation Solver programı (EES) kullanılarak yapıldı. İlk olarak, bu çalışmada kullanılan Beş Organik çalışma sıvısı, ikinci aşama R410a sabiti ve birinci aşama R32, R227ea, R410a, R290 ve R134a çalışma sıvıları olarak belirli bir sıcaklık limitleri için kullanılmıştır. Bu çalışmanın amacı, çalışma akışkanının sistem verimliliğine etkisini belirlemek ve en uygun çalışma akışkanı çiftini bulmaktır. İkinci olarak, birinci ve ikinci aşamalarda sekiz farklı organik çalışma sıvısı (R134a, R410a, RC318, R407c, R22, R23, R116 ve R218) belirli sıcaklık limitleri için çiftler halinde kullanılmıştır. Uygun bir soğutucu veya soğutucu çifti seçmek, ORC'nin yüksek termal verimliliği ve net iş çıkış değeri için çok önemlidir. Bu çalışma, çalışma akışkanının sistem verimliliğine etkisini belirlemeyi ve en uygun çalışma akışkanı çiftini bulmayı amaçlamaktadır. Son olarak, belirli sıcaklık limitleri için birinci ve ikinci aşamalarda soğutucu olarak R245fa kullanılmaktadır. Çalışmanın amacı, çalışma sıcaklığının sistem verimliliğine, ekserji verimliliğine etkisini belirlemek ve en uygun çalışma sıcaklığını bulmaktır.

Sonuçlar, ilk çalışma, R227ea + R410a çiftinin en yüksek termal verimi verdiğini ancak en yüksek net güç çıkışının R290 + R410a soğutucu akışkan çiftlerinden elde edildiğini göstermiştir. R410a ikinci aşama için sabittir ve R134a, R32, R410a, R290, R227ea birinci aşama için değiştirilir. Sıcaklık arttığında R227ea + R410a, R290 + R410a ve R134a + R410a çiftlerinin termal veriminin düştüğü açıkça görülmektedir. Ayrıca R290 + R410a çifti, R32 + R410a çiftine göre %28.9 daha yüksek net güç çıkışı verdi. Ve R227ea + R410a çifti en küçük net güç çıkışını verdi. R32 + R410a çifti, R134a + R410a çiftine göre %41 daha fazla güç çıkışı sağlar. İkinci hesaplama, en yüksek net güç çıkışının ve en yüksek termal verimliliğin R23 + R23 çiftinden elde edildiğini gösterdi. ORC sisteminde R23 + R23 çifti kullanıldığında ve türbin giriş sıcaklığı 425 K olduğunda, termal verim R22 + R22 çiftinden %4.31 daha fazladır. R23 + R23, R22 + R22, R410a + R410a ve R407c + R407c soğutucu çiftleri kullanıldığında sistemin termal verimliliği sıcaklıkla artar. Tüm soğutucu akışkanlar arasında, tüm çalışma sıcaklıkları için R23 önerilebilir. Çünkü R23 + R23 çifti tüm sıcaklıklar ve çalışma akışkanları için en yüksek net güç çıkışı ve termal verim değerlerini verir. Sıcaklık arttığında diğer çiftlerin ısıl verimi azalır. Öte yandan, R218 + R218 çifti kullanıldığında, tüm sıcaklıklarda diğer çiftler arasında en küçük sistem ısıl verim değeri elde edilmiştir. RC318 + RC318 çiftinden gelen en düşük net güç çıkışının türbin giriş sıcaklığını arttırarak RC318 + RC318 çiftinin termal verimini olumsuz etkilediği de gözlemlenmiştir. Bu termal verim, 6.708'den 5.338'e önemli ölçüde düşer. R22, R407c, R410a ve R23'ün ısıl veriminin sıcaklık arttıkça arttığı gözlemlenmiştir. Diğer soğutucu akışkanlarda ise sıcaklık arttıkça ısıl verimler düşmüş ve en düşük ısıl verim R218 + R218 çiftinden elde edilmiştir. Evaporatör giriş sıcaklığının artmasıyla çevrimin ekserji verimliliği azalır. Aynı zamanda, artan evaporatör giriş sıcaklığı ile sistemin ısıl verimi düşmektedir. En yüksek termal ve ekserji verimleri 400K sıcaklıkta görülür. Türbin1 ve 2 için evaporatör giriş sıcaklığına karşı ekserji verim ve ekserji yıkım değerleri. Türbin-1'deki en küçük ve en yüksek ekserji kayıpları sırasıyla 0,4514 kW ve 0,6653 kW'dır. Türbin-1'deki ekserji veriminin yüzdesi 400K ve 425K için sırasıyla 98.14 ve 97.54'tür. Evaporatör giriş sıcaklığı arttığında Türbin-2'deki ekserji verimi azalırken, türbin-2'deki ekserji yıkımı artar. Türbin-2'deki en küçük ve en yüksek ekserji yıkımı sırasıyla 0.1258 kW ve 0.1496 kW'dır. Türbin-2'deki ekserji veriminin yüzdesi 400K ve 425K için sırasıyla 99.25 ve 98.48'dir. Pompa1 ve 2 için sıcak akışkanın evaporatör giriş sıcaklığı arttıkça ekserji verimi düşmektedir. Ayrıca evaporatör giriş sıcaklığı 400K olduğunda en yüksek ekserji verimi Pompa-1 ve 2 için sırasıyla %6,18 ve %83 olarak hesaplanmıştır. Pompa 1 ve 2 için ekserji verim değerleri %5,48 ve %44'e kadar düşmektedir. En büyük verimler Türbin1 ve 2'de ve Evaporatörde elde edilmiştir. Hem Kondenserlerde hem de Pompa1'de en düşük verimlilik elde edildi. Tüm sıcaklıklar için diğer bileşenlere kıyasla Pompa1'de maksimum ekserji yıkımı bulunur. Tüm sıcaklıklar için diğer bileşenlere kıyasla Türbin2'de minimum ekserji yıkımı bulunur. 405K'da çalışan farklı soğutucu akışkanlar için kondenser 1 ve 2 çıkış sıcaklık değerleri. R23 + R23 çiftleri, sırasıyla 218.7K ve 190.9K olan en küçük kondenser 1 ve 2 çıkış sıcaklıklarını verir. Aynı çalışma koşulunda R245fa + R245fa çiftleri, sırasıyla 328K ve 288K olan en yüksek kondenser 1 ve 2 çıkış sıcaklıklarını verir. Yani atmosfer koşullarında çalışan ORC'ye göre R245fa + R245fa çiftleri uygundur, çünkü çiftler sırasıyla 328K ve 288K olan en yüksek kondenser 1 ve 2 çıkış sıcaklıklarını verir.

ACKNOWLEDGEMENTS

I would like to thank my supervisor Assoc.Prof.Dr. Arif ÖZBEK who continuously supported and guided my thesis work. Also, I would like to express my gratitude to Prof. Dr. Hüseyin AKILLI for his support and encouragement as the Head of the Mechanical Engineering Department.

I would like to thank Research Assistant Sergen TÜMSE and Research Assistant Atakan TANTEKİN for their invaluable assistance during my experiments.

I would like to express my special thanks to my mother, Ayşe KAPLAN, and my sister, Hürü KAPLAN, who was with me during my master studies, sharing my hard days, and giving me strength with their presence.

I would like to express my special thanks to my fiancée, Selin YILDIRIM who was sharing my sadness and joy, and giving me strength with her presence.

I express my deepest gratitude especially to my friend Bektaş KARAKOYUN who have continuously encouraged me along the way of my M.Sc.

Thank you so much to everyone who shared this journey with me.

CONTENTS **PAGES**

LIST OF FIGURES **PAGES**

LIST OF TABLES **PAGES**

XVII

NOMENCLATURE

h	: Enthalpy [$kjkg^{-1}$]
$\dot{m}$	: mass flow rate [kgs^{-1}]
$\dot{Q}$	: heat transfer rate [kW]
C	: heat capacity rate [$kW^{o}C^{-1}$]
T	: temperature [^{o}C or K]
$\dot{W}$	: work [kW]
A	: surface area [m^2]
Abbreviations	
ORC	: Organic Rankine Cycle
EES	: Engineering Equation Solver
p	: Pump
out	: Outgoing
in	: Incoming
r	: Re-evaporator
T	: Turbine
Th	: Thermal
Min	: Minimum
Max	: Maximum
Act	: Actual
M	: Mechanic
H	: Hot
C	: Cold
Subscripts	
I	: upper stage
II	: lower Stage
Greek symbols	
η	: efficiency

1. INTRODUCTION

Power generation from waste heat, turbine exhaust, solar and biomass energy is becoming a popular way to generate alternative energy for industry. Low heat sources can be converted to electrical energy and these can be used in an organic rankine cycle system design. Egelioğlu and Obafunmi (2014) described basic principles of organic rankine cycle, very similar to the conventional Rankine cycle. However, the main difference is the use of organic working fluid of the organic rankine cycle.

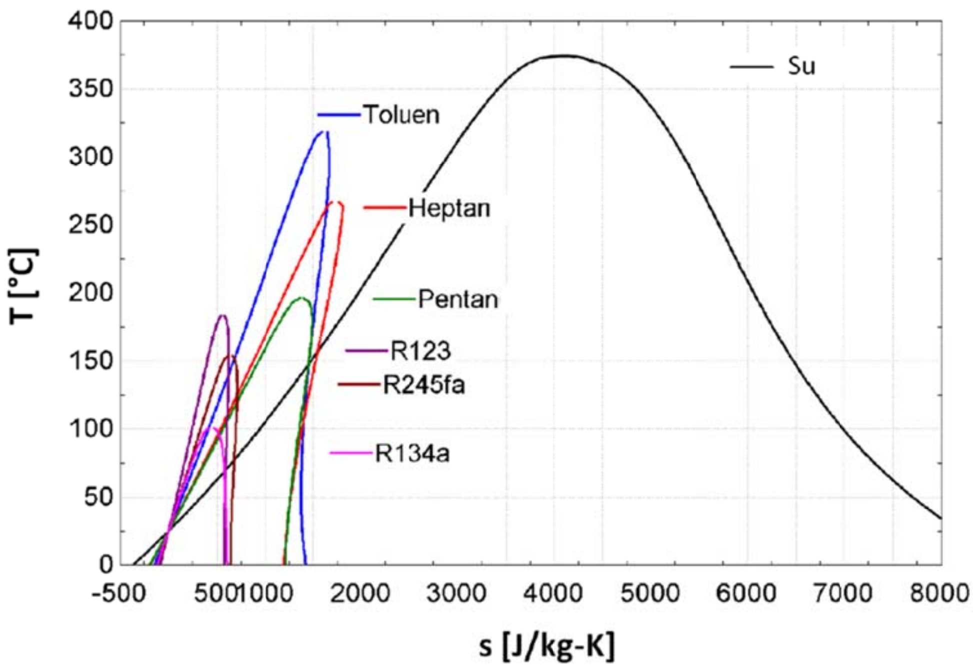

Figure 1.1. Temperature-entropy diagrams of some working fluids and water used in ORC.

Quoilin et al. (2011) worked on rankine cycle requires minimum power to be competitive and high collector temperature. The main problems for generating power economically with water/steam driven working cycles is that low (<230 °C) and medium (230°C - 640°C) temperature heat sources are not suitable (Becquin and Lehar, 2012). Also Wali (1980) worked on when using water as a working fluid, many problems are encountered: during expansion need of superheating to prevent condensation, excess pressure in the evaporator, risk of erosion of turbine blades, expensive and complex turbines. Various cycles such as organic Rankine, supercritical Rankine, Kalina, Goswami and triple flash cycles have been investigated for the generation of electrical energy from low temperature heat sources (Davidson, 1977). However, organic rankine cycle s have a much simpler cycle than other cycles such as the Kalina cycle or triple flash cycles (Chen et al., 2010). Compared to the conventional Rankine cycle with organic rankine cycle, they require a less complicated control system and their components are a lot cheaper.

The term exergy was first used by Carnot in 1824 (Wall, 1998). Studies on exergy analysis started with Gouy and Stodola. At the beginning of this century, scientists such as Jouguet, Lewiss and Randall, DeBaufre, Darrieus, Keenan, Lerberghe and Glansdorf made great contributions to the development of thermodynamics and the concept of exergy; In 1935, Bosnjakovic started to apply the concept of exergy to the thermodynamic analysis of systems (Rivero and Anaya, 1997).

Exergy is defined as the maximum work that can be obtained from a system by bringing it under the same conditions as the environment (Kotas, 1995). When a system is dead state, it is at the same temperature and pressure as its surroundings. In other words, it is in thermal and mechanical or thermodynamic equilibrium with the environment. Also, the kinetic and potential energies of the system with respect to its surroundings are zero. When the system is dead state, it cannot enter into a chemical reaction with its environment. The dead state properties of the system are P_0, T_0, h_0, u_0 and S_0. At dead state P_0= 1 atm (101.325 kPa) and T_0=25 °C (298.15 K) (Çengel and Boles, 1998). The work potential of the systems will be characterized by exergy analysis. It provides a more realistic view of various devices and processes. Most thermodynamic systems possess energy, entropy, and exergy, and in this way appear at the intersection of these three fields (Cengel and Dincer, 2001).

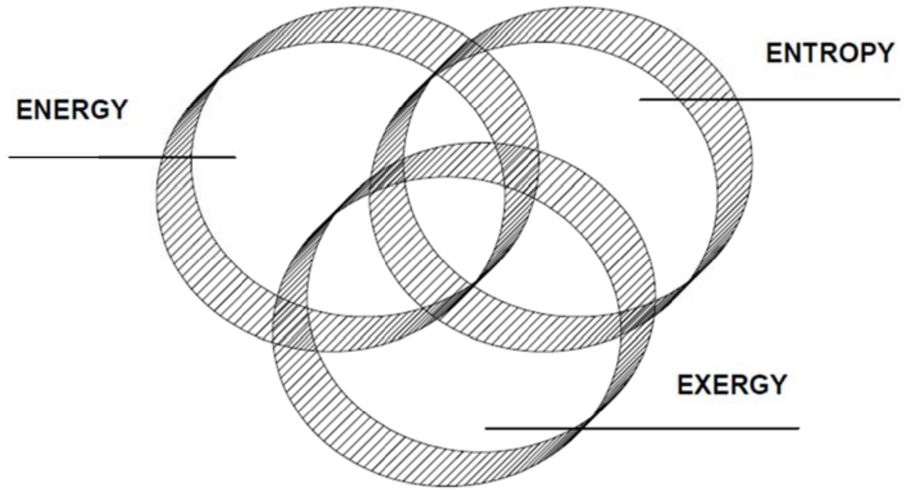

Figure 1.2. Interactions between the domains of energy, entropy and exergy.

In this thesis, 3 type of calculation is done. First, Different Refrigerant at First Stage and R410a at Second Stage. The aim of this study, a thermodynamic model of the ORC that can work with different refrigerants has been constructed. While the working fluid in the second stage was kept constant, the effects of the working fluid on the system performance in the first stage were investigated. System thermal efficiency and net power output were calculated according to working fluid couple and temperature. Second, Same Refrigetants at Two Stage for Different Working Fluid Pairs. This study's aim, energy analysis of a double-stage Organic Rankine Cycle (ORC) was performed using the Engineering Equation Solver program (EES). In the first and second stages, R134a, R410a, RC318, R407c, R22, R23, R116 and R218 organic fluids were used in pairs for certain temperature limits. In order to obtain the best thermal efficiency and network output value from ORC to find out, a suitable fluid or fluid pair has been tried to determine. Third, R245fa at Two Stage for Different Working Temperatures**.** This study aims to determine the effect of working temperature on system efficieny, exergy efficiency and find out the most suitable working temperature. As a resoult, energy and exergy analysis of a double-stage Organic Rankine Cycle (ORC) was performed using the Engineering Equation Solver program (EES). In the first and second stages, Twelve Organic working fluids used in R32, R227ea, R410a, R290, R134a, RC318, R407c, R22, R23, R116, R218 and R245fa. In order to obtain the best thermal efficiency, net work output value and useful refrigerant fluid for environmental situation a suitable fluid or fluid pair has been tried to determine.

2. PREVIOUS STUDIES

In 1825 Thomas Howard developed the first organic rankine cycle engines. The working fluid was alcohol or ether. In 1967, the Soviet Union's first geothermal binary organic rankine cycle was developed on the Kamchatka peninsula. The capacity was 680 kW and the working fluid was R-12 (Lee, 2014).

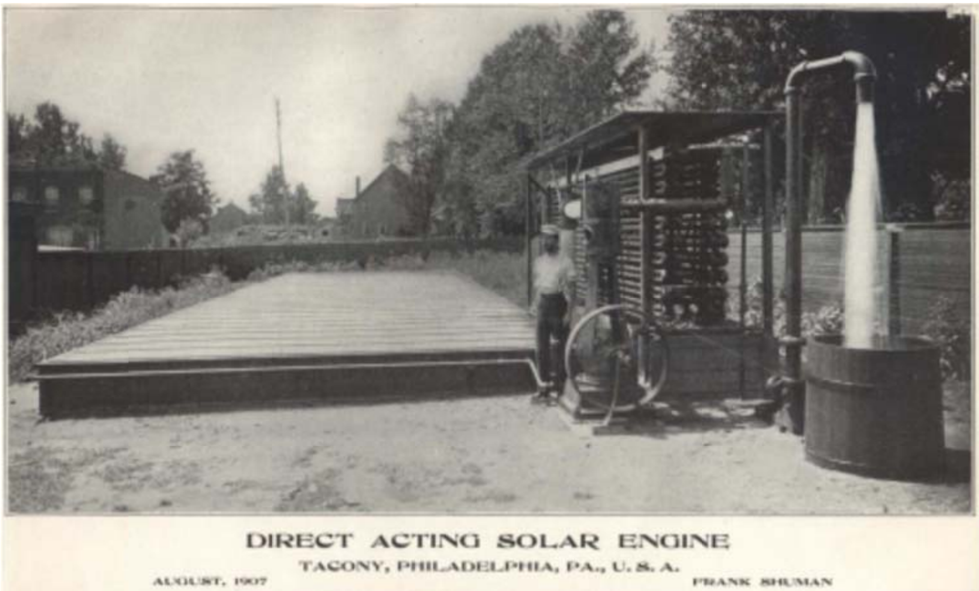

Figure 2.1. A flat solar collector which is produced by Frank Shuman, in 1907 used.

Eyidogan et al. (2016) stated that Organic rankine cycle technology is a promising and proven technology that is considered an essential solution for low and medium temperatures (especially between 300–450 °C). Low-temperature heat is converted into useful work, which itself can be converted into electricity. Joshi et al. (2011) indivated that usually, renewable energy resources are sustainable. Sun is the main source of energy on earth. Solar energy heats up the surface of the world. Hence, these renewable energy can be used.

Lim et al., (2017) worked on and listed the advantage of organic rankine cycle is that various working fluids can be used first. Second, the working fluid is mostly dry fluid. Third, the working fluid has a relatively low evaporation temperature. Organic rankine cycle also has disadvantages, one of which is its poor heat transfer coefficient. Second, most organic liquids are poisonous and highly flammable. Therefore, the “shell and tube” type heat exchanger is easily adopted in the organic rankine cycle system. Wang et al., (2020) explained that numerous researchers have extensively studied the organic Rankine Cycle, focusing mainly on system structure, working fluid, and optimization of cycle parameters. Bertrand et al., (2009) indicated that the refrigerants studied found that the organic rankine cycle 's most suitable working fluid for small-scale solar applications was R134a.

Tchanche et al. (2008) stated that a bad working fluid choice could lead to a low efficient and expensive plant. That means suitable fluid should have properties of high efficiency, low specific volumes and moderate pressures in the heat exchangers, low toxicity, low cost, low Ozone Depletion Potential (ODP) and low Global Warming Potential (GWP), among others (Maizza and Maizza, 1996). According to Borsukiewcz-Gozdur and Nowak, (2007) the selection of the working fluid is determined by the application and the waste heat level and plays a significant role in the use of the organic rankine cycle process. Organic fluid can operate at much lower evaporation temperature and pressure than a conventional turbine and still perform at high efficiency (Drescher and Bruggemann, 2007). According to Salih et al. (2007) they investigated 31 components working for subcritical and supercritical organic rankine cycle s for geothermal power plants. The second category examined is the use of solar energy. Wang.et al. designed a experimental set up rankine cycle of solar operated by using R245fa as a working fluid and used evacuated and flat plate collector. He found the efficiency of with flat plate collector is 3.2 % and overall power generation of evacuated collector is 4.2%. Dincer and Rosen (2005) indicat that exergy is usually not conserved as energy, it is destroyed in the system. Exergy analysis is useful for increasing the efficiency of energy use, as it quantifies the types of locations and the magnitudes of losses and wastes. In general, more meaningful efficiencies are evaluated through exergy analysis because exergy efficiencies are always a measure of how close a process's efficiency is to the ideal. Therefore, exergy analysis accurately identifies the available margin to design more efficient energy systems by reducing inefficiencies. In exergy analysis, the reference state needs to be defined by specifying the temperature, pressure, and chemical composition. Such a reference environment or reference state must be defined before starting the analysis. Surrounding ambient conditions are often considered reference or dead state conditions. When performance is evaluated, it becomes dependent on the dead state (Dincer and Rosen, 2007).

Wang et al. (2012) analyzed a power plant operating under supercritical conditions using advanced exergy analysis and suggested appropriate optimization strategies. That suggestion is improve the generator first, then the turbines. A waste heat powered organic Rankine cycle was analyzed by Kaska (2014) and assessed performance of the cycle and pinpoint sites of primary exergy destruction using actual plant data. Tsatsaronis and Park (2002) analyzed the effects of avoidable and unavoidable exergy consumptions in the thermodynamic analysis of heat systems and cost analysis of system components in their study based on the cogeneration system. They emphasized that special attention should be paid to avoidable exergy consumption and investment costs can be reduced by defining the parts of exergy consumption that can be reduced. Cengel and Boles (2010) indicated that in thermodynamic analysis, the energy equation alone is insufficient to evaluate flat plate solar collector efficiency. To increase the efficiency of the system exergy analysis is more effective for determining the source and magnitude of irreversibility. According to the ambient temperature exergy is the maximum output that can be obtained.

El-Emam and Dinçer (2013) conducted thermodynamic and economic analyzes on a new type of geothermal regenerative organic Rankine cycle based on both energy and exergy concepts. The energy and exergy efficiency values for the geothermal regenerative organic Rankine cycle were found to be 16.37% and 48.8%, respectively. A cost-optimal design criterion was presented by Madhawa et al. (2007) for a simple organic rankine cycle power cycle using a low-temperature geothermal resource. Wang and Dai (2016) worked on the performance of two different cycles using exergoeconomic optimization and also compared the outcomes of the cycles they considered for different working fluids. The outcomes showed that the total product unit cost for the combination of supercritical CO_2 Brayton and ORC cycles was marginally lower than for the combination of supercritical CO_2 Brayton and transcritical CO_2 cycles.

3. MATERIAL AND METHOD

3.1. System Description

Figure 3.1 shows the double stage ORC system designed. In this system, the solar collector acts as a heater. The evaporator of the first stage takes the heat from the solar collector and delivers that heat to the working fluid of the first stage. After the turbine-I, the fluid is still in the superheated gas state and this heat is used as the second-stage working fluid in a Re-evaporator. After the turbine-II, the regenerator heats the compressed liquid as a pre-heater. The water is used as a cooler at both condensers.

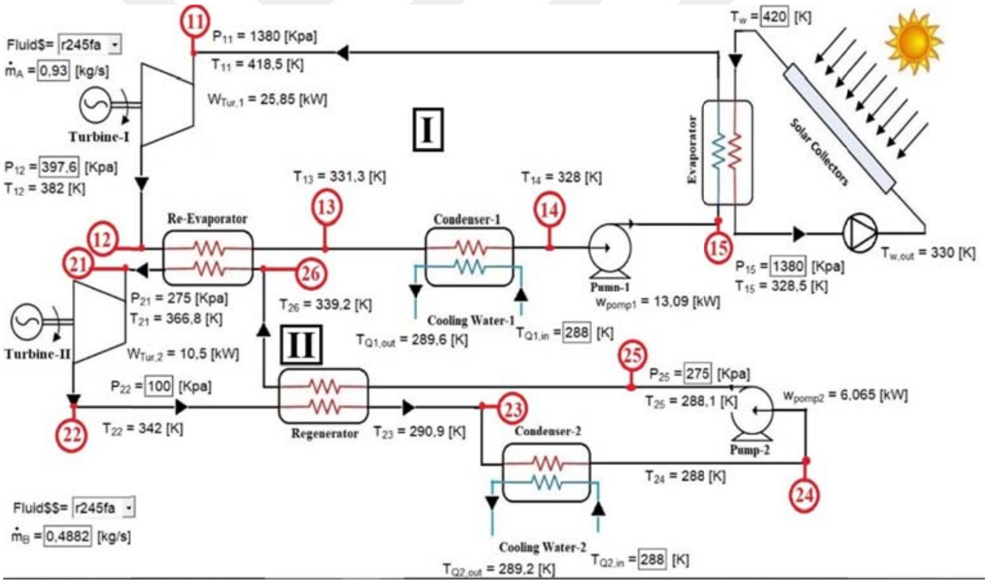

Figure 3.1. Schematic representation of Double Stage SORC system.

This system consists of two stages. In the first and second stages, the same fluid is used and the heat taken from the solar collector is converted into electrical energy. Solar collector can be change with all of the heat sources like geothermal energy, natural gas, waste heat, etc.. The system operates with a constant mass flow rate of 0.93 kg/s and 0.4882 kg/s in the first and second stages, respectively. In addition, the working pressure is constant in all components and refrigerant pairs. Calculations were made between, the lowest temperature at which all fluids can work together, and the highest temperature at which they can work.

Figure 3.2 illustrates the pressure/enthalpy diagram of the double-stage Rankine cycle designed with R2245fa at each stage. The points in the first stage show: 11-12 is the turbine, 12-13 is the re-evaporator, 13-14 is a condenser, 14-15 is a pump, and 15-11 is the evaporator where heat is gained from the solar collector. The points in the second stage show: 21-22 is a turbine, 22-23 is a regenerator, 23-24 is a condenser, 24-25 is a pump, and 25-21 is an evaporator where heat is gained from re-evaporator.

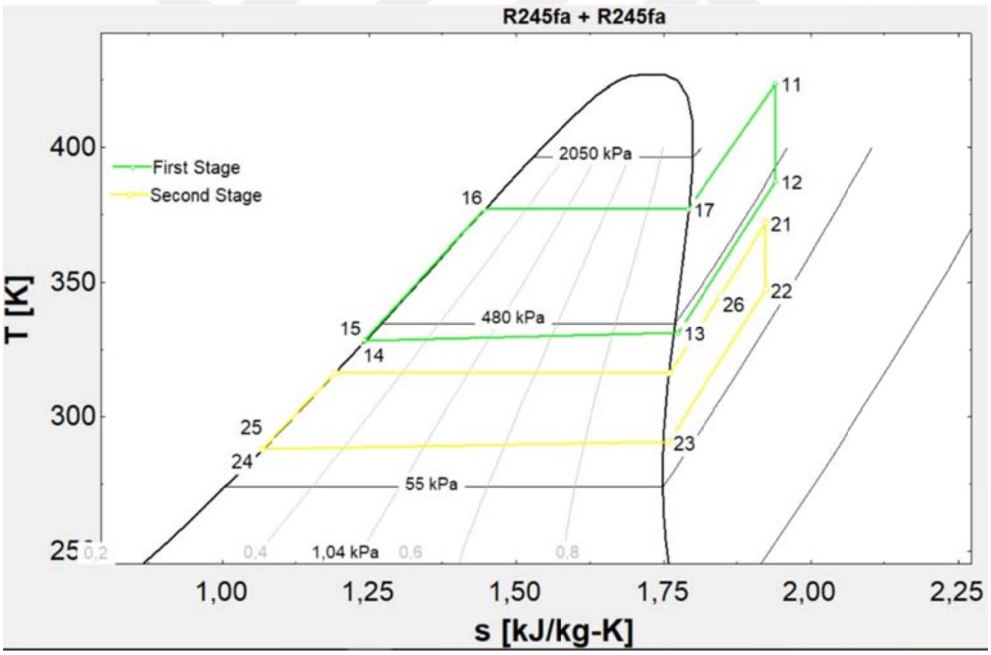

Figure 3.2. Pressure/enthalpy chart of double-stage Rankine cycle with R245fa at each stage.

3.2. Organic Refrigerants

Good working fluid should have a low steam and low liquid specific volume (Badr et al., 1985). The specific volume of the fluid pressure in the condenser should be as small as possible to minimize the required feed pump work (Bertrant et al., 2008). Table 3.1 shows physical, safety and environmental data of the working fluids used in the analyses.

Table 3.1. Physical, safety and environmental data of the working fluids

Substance	**Molecular Mass (kg/kmol)**	**T_{bp} (^oC)**	**T_{cr} (^oC)**	**P_{cr} (MPa)**	**ASHRAE 34 Safety Group**	**Atmospheric life time (yr)**	**ODP**	**GWP (100 yr)**
R134a	102.03	-26.1	101.1	4.06	A1	13.4	0	1370
R410a	72.58	-51.4	71.4	4.90	A1	-	0	2100
RC318	200.03	-6.0	115.2	2.778	A1	3200	0	10250
R407C	86.20	-43.6	86.8	4.597	A1	n.a	0	1800
R22	86.47	-40.8	96.1	4.99	A1	11.9	0.040	1790
R23	70.01	-82.0	26.1	4.83	A1	222	0	14200
R116	138.01	-78.1	19.9	3.05	A1	10000	0	12200
R218	188.02	-36.8	71.9	2.64	A1	2600	0	8830
R32	52.02	-51.7	78.11	5.784	A2	4.9	0	675
R227ea	170.03	-16.3	101.8	2.93	A1	38.9	0	3580
R290	44.10	-42.1	96.68	4.247	A3	0.041	0	~20
R245fa	134.05	15.3	154.1	3.64	B1	8.8	0	820

T_{bp}: Normal boiling point; T_{cr}: Critical temperature; P_{cr}: Critical pressure; ODP: Ozone depletion potential, relative to R-11; GWP: Global warming potential, relative to CO_2. n.a: non available.

3.3. ASHRAE 34 Refrigerant Safety Classification

According to ASHRAE 34 Refrigerant Safety Classification group A, all refrigerants have been determined, which means low toxicity and no flame propagation group. ASHRAE 34 refrigerant safety classification is shown in Table 3.2. The first stage's working fluid and the second stage's working fluid have been set as the same refrigerant. The effectiveness–NTU method is used to model the Evaporator and Re-evaporator heat exchangers.

Table 3.2. ASHRAE 34 Refrigerant Safety Classification

	Lower toxicity	**Higher toxicity**
Higher flammability	A3	B3
Lower flammability	A2	B2
No flame propagation	A1	B1

According to the ASHRAE standard 34, there are two classes of toxicity (**A**: non-toxic **B**: toxic.) and three groups of flammability characteristics (**1**: no flame propagation, **2**: low flammability limit and **3**: high flammability limit) (Bertrant et al., 2008).

3.4. Thermodynamic Analysis

Rankine cycles with four components (pump, boiler, turbine and condenser) are constant-flow devices and therefore, all arithmetic operations constituting the Rankine cycle can be analyzed as the fixed-flow process. Kinetic and potential energy, work, and is small compared to the heat transfer terms are often ignored (Cengel and Boles, 2005).

3.4.1. Energy Analysis

It is assumed that the pump and turbine are isentropic. The boiler and condenser do not require any work. Then the conservation of energy relationship for each device can be expressed as:

Stage -I Processes:

Process 11 - 12 is the actual expansion process in the Turbine-I.

$$\dot{W}_{T-I} = \dot{m}_I \times (h_{11} - h_{12}) \times \eta_m \tag{1}$$

The isentropic efficiency of Turbine-I is η_{T-I}=0.8 at the designed condition.

Process 12 – 13 is the desuperheated process with Re-evaporator.

$$\dot{Q}_r = \dot{m}_I \times (h_{12} - h_{13}) \tag{2}$$

Process 13 – 14 is the condensation process.

$$\dot{Q}_{out-I} = \dot{m}_I \times (h_{13} - h_{14}) \tag{3}$$

Process 14 – 15 is the pumping process.

$$\dot{W}_{p-I} = \dot{m}_I \times (h_{14} - h_{15}) \times \eta_p \tag{4}$$

The pump efficiency is η_{p-I} =0.8 at the designed

Process 15 – 11 is the heating process by a solar collector.

$$\dot{Q}_{in} = \dot{m}_I \times (h_{11} - h_{15}) \tag{5}$$

Stage-II Processes:

Process 21 - 22 is the actual expansion process in the Turbine-II.

$$\dot{W}_{T-II} = \dot{m}_{II} \times (h_{21} - h_{22}) \times \eta_{T-II} \tag{6}$$

The isentropic efficiency of an turbine is η_{T-II} =0.8 at the designed condition.

Process 22 – 23 is the Regenerator process.

$$\dot{Q}_{R-II} = \dot{m}_{II} \times (h_{22} - h_{23}) \tag{7}$$

When the heat source temperature is relatively high, the ORC with a regenerator is better than the basic ORC (Li et al.,2018).

Process 23 – 24 is the condensation process.

$$\dot{Q}_{out-II} = \dot{m}_{II} \times (h_{23} - h_{24}) \tag{8}$$

Process 24 – 25 is the pumping process.

$$\dot{W}_{p-II} = \dot{m}_{II} \times (h_{24} - h_{25}) \times \eta_{p-II} \tag{9}$$

The pump efficiency is η_{p-II} =0.8 at the designed condition.

Process 25 – 21 is the heating process by Re-evaporator.

$$\dot{Q}_{in-II} = \dot{m}_{II} \times (h_{21} - h_{25}) \tag{10}$$

The net electrical power produced by the system is calculated from equation (11).

$$\dot{W}_{net} = \left(\dot{W}_{T-I} + \dot{W}_{T-II}\right) - (\dot{W}_{p-I} + \dot{W}_{p-II}) \tag{11}$$

The thermal efficiency of the double stage ORC system is determined from equation (12):

$$\eta_{th} = \frac{\dot{W}_{net}}{\dot{Q}_{in}} \tag{12}$$

The effectiveness – NTU Method:

The effectiveness – NTU method was found in Kays and London in 1955. This method greatly simplified heat exchanger analysis (Klein, 2003). All heat exchangers are calculated by the ε-NTU:

$$\varepsilon = \frac{\dot{Q}_{act}}{\dot{Q}_{max}} \tag{13}$$

ε is the heat transfer effectiveness which is a dimensionless parameter. Defined as; the ratio of actual heat transfer rate to maximum possible heat transfer rate.

To determine the maximum possible heat transfer rate in a heat exchanger, maximum temperature difference in a heat exchanger is the difference between the inlet temperature of the hot and cold fluids (Cengel, 2002).

$$\dot{Q}_{act} = C_h(T_{h-in} - T_{h-out}) = C_c(T_{c-out} - T_{c-in}) \tag{14}$$

C_h and C_c are the heat capacity of the hot and cold fluids, respectively.

$$\dot{Q}_{max} = C_{min}(T_{h-in} - T_{c-in}) \tag{15}$$

The C_{min} is the smaller fluid thermal capacity. The U is the overall heat transfer coefficient.

$$NTU = \frac{U \times A}{C_{min}} \tag{16}$$

NTU is a dimensionless number which means number of transfer unit.

3.4.2. Exergy Analysis

Exergy is a measure of a system's capacity to do useful work as it progresses to a certain end state in equilibrium with its environment. Exergy is usually not conserved as energy, it is destroyed in the system. Exergy destruction is a measure of irreversibility that is the source of performance loss. Therefore, an exergy analysis that assesses the magnitude of exergy destruction identifies the location, magnitude, and source of thermodynamic inefficiencies in a thermal system (Aljundi, 2009).

For process components the following exhibits the numerous rate balance values based on energy and exergy approaches. The equations for a steady-state system are given below (Kaushik, 2011).

$$\sum \dot{m}_i = \sum \dot{m}_e \tag{17}$$

$$Q - W = \sum E_e - \sum E_i \tag{18}$$

$$X - W = \sum X_e - \sum X_i + X_D \tag{19}$$

The general exergy balance is expressed in the rate form as:

$$\dot{E}X_i - \dot{E}X_e = \dot{E}X_D \tag{20}$$

And on a unit mass basis, the specific exergy is calculated as:

$$ex = h - h_0 - T_0(s - s_0) \tag{21}$$

Table 3.3 shows exergy analysis equations for all the system components.

Table 3.3. Exergy analysis equations for the system components

Stage	Components	Exergy destruction rate	Exergy efficiency
S-I	Turbine-1	$X_D = X_{11} - W_{T1} - X_{12}$	$n_{t1} = \frac{W_{T1}}{X_{11} - X_{12}}$
	Condenser-1	$X_D = X_{13} + X_{cw1\text{-}in} - X_{14} - X_{cw1\text{-}out}$	$n_{c1} = \frac{X_{cw1-in} - X_{cw1-out}}{X_{13} - X_{14}}$
	Pump-1	$X_D = X_{14} + W_{P1} - X_{15}$	$n_{p1} = \frac{X_{15} - X_{14}}{W_{P1}}$
	Evaporator	$X_D = X_{15} + X_{SC\text{-}in} - X_{11} - X_{SC\text{-}out}$	$n_{evap} = \frac{X_{11} - X_{15}}{X_{SC-in} - X_{SC-out}}$
S-I & S-II	Re-Evaporator	$X_D = X_{12} + X_{26} - X_{13} - X_{21}$	$n_{R-e} = \frac{X_{12} - X_{13}}{X_{26} - X_{11}}$
S-II	Turbine-II	$X_D = X_{21} - W_{T2} - X_{22}$	$n_{t2} = \frac{W_{T2}}{X_{21} - X_{22}}$
	Condenser-II	$X_D = X_{23} + X_{cw2\text{-}in} - X_{24} - X_{cw2\text{-}out}$	$n_{c2} = \frac{X_{cw2-in} - X_{cw2-out}}{X_{23} - X_{24}}$
	Pump-II	$X_D = X_{24} + W_{P2} - X_{25}$	$n_{p2} = \frac{X_{25} - X_{24}}{W_{P2}}$
	Regenerator	$X_D = X_{22} + X_{25} - X_{23} - X_{26}$	$n_{Rg} = \frac{X_{22} - X_{23}}{X_{25} - X_{26}}$

3.4.3. Exergoeconomic Analysis

Exergoeconomics is based on the concept of exergy, which is the only rational basis on which thermodynamic inefficiencies in and around an energy conversion system can be associated with monetary costs. This approach is called exergy costing by Tsatsaronis (1999). Exergy costing is also called exergoeconomics. In some cases, the different term “thermoeconomics” is also used interchangeably with exergoeconomics. (Tsatsaronis, 1999). The goal is not just to calculate the cost of one or more products, but rather to understand the process of cost escalation through the conversion and depreciation of energy, which is defined by the gradual decline of exergy.

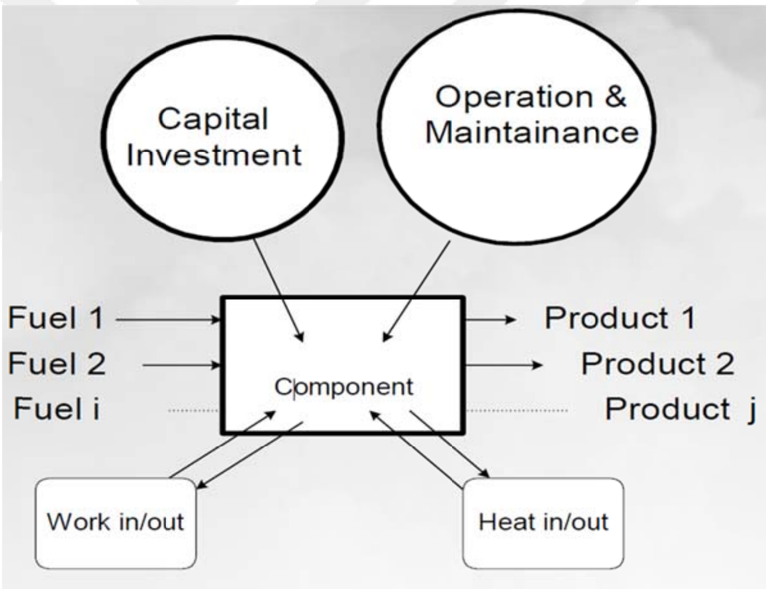

Figure 3.3. Exergoeconomic of Capital Investment.

To calculate an exergoeconomic analysis, a cost balance equation along with enough number of auxiliary equations, are applied to each system component. The cost balance equation is (Bejan et all.,1996);

$$\sum \dot{C}_{out,k} = \sum \dot{C}_{in,k} + \dot{Z}_k \tag{22}$$

In this equation $\dot{C}$ is the cost rate associated with the inlet and outlet exergy streams and $\dot{Z}$ is the total cost ratio of capital investment and operation and maintenance costs for the kth component. The cost rates expressed with the power, heat and the stream of matter can be written as a function of specific exergy costs as follows:

$$\dot{C}_i = \dot{c}_i \dot{E}_i \tag{23}$$

$$\dot{C}_w = \dot{c}_w \dot{W} \tag{24}$$

$$\dot{C}_q = \dot{c}_q \dot{E}_q \tag{25}$$

The $\dot{Z}$ term for the kth component can be expressed as:

$$\dot{Z}_k = \dot{Z}_k^{CI} + \dot{Z}_k^{OM} \tag{26}$$

4.RESULTS AND DISCUSSION

4.1. Different Refrigerant at First Stage and R410a at Second Stage

For R410a as being refrigerant at first and second stage thermodynamic properties were calculated by EES (Engineering Equation Solver) software program. Refrigerants was changed and effect on system at same condition was calculated.

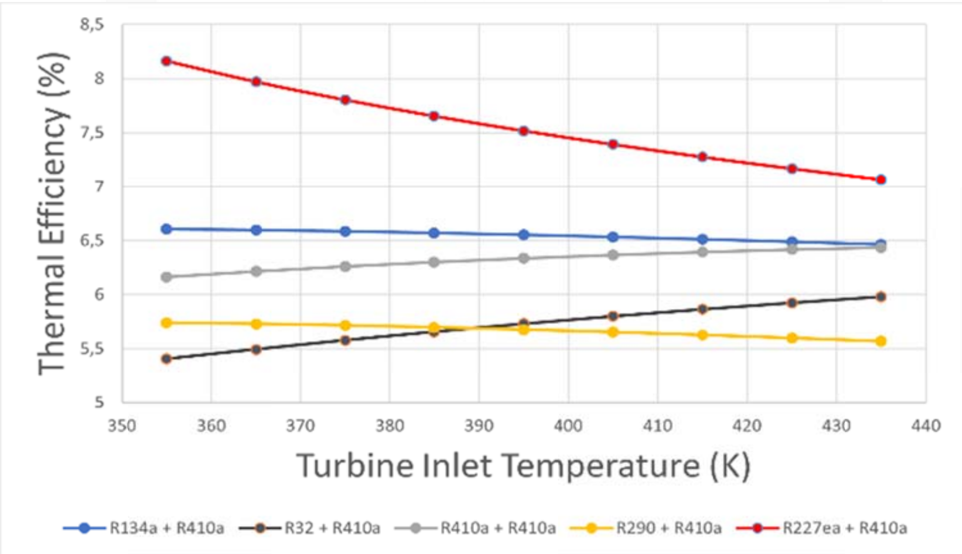

Figure 4.1. System thermal efficiency for different refrigerant at first stage and R410a at second stage.

Figure 4.1 shows the variation of different working fluids at first stage when R410a refrigerant at second stage. R410a is constant for second stage and R134a, R32, R410a, R290, R227ea is changed for first stage. It is clearly seen that thermal efficiency R227ea + R410a, R290 + R410a and R134a + R410a couples decreases when the temperature is increased.

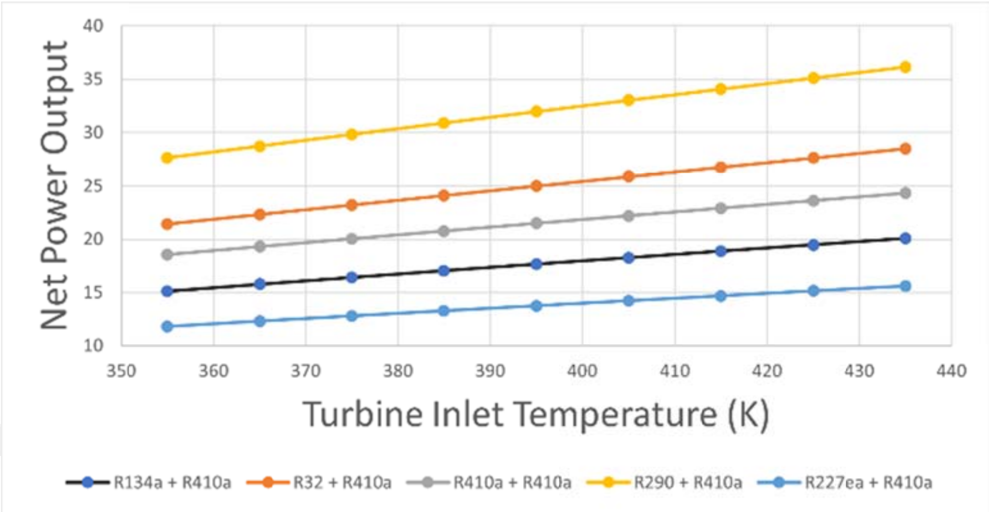

Figure 4.2. System net power output according to different couple and temperature.

Figure 4.2 shows the net power output changes according to turbine inlet temperature. R290 + R410a couple gave the %28.9 higher net power output then R32 + R410a couple. And R227ea + R410a couple gave the smallest net power output.

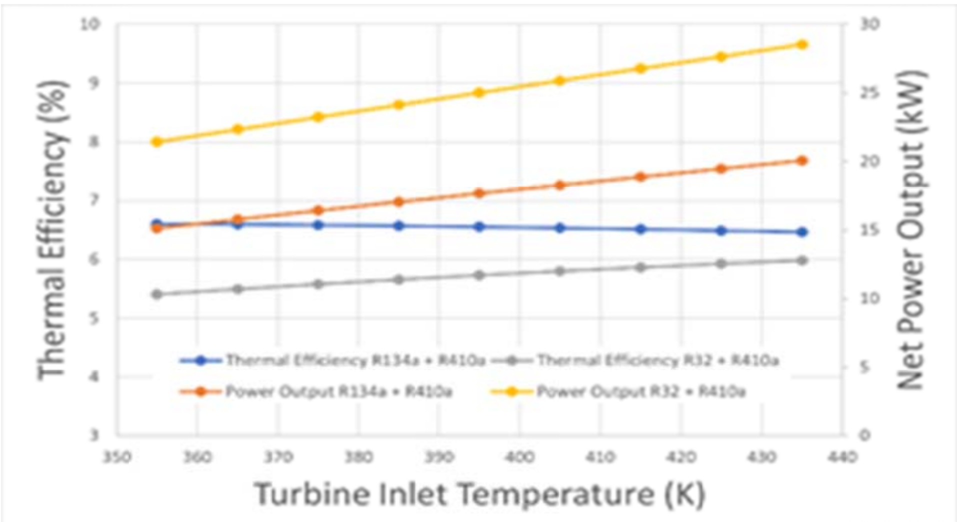

Figure 4.3. System net power output and thermal efficiency at same temperature

Figure 4.3 shows the R134a + R410a and R32 + R410a couple's thermal efficiency and net power output according to various temperature. R32 + R410a couple gave %41 higher net power output and thermal efficiency of this couple is increasing according to temperature is increased.

4.2. Same Refrigetants at Two Stage for Different Working Fluid Pairs

Thermodynamic properties of the R23 refrigerant in the first and second stages were determined with the EES (Engineering Equation Solver) software program. EES simplifies the process and is the assurance that the solver will operate at optimum efficiency. EES automatically identifies and groups equations that need to be solved and uses equations instead of assignments normally used in formal programming languages (Klein, 2003)

The effect on the system in the same situation is calculated by changing the refrigerant pair and turbine inlet temperature (T_{11}).

For Turbine Inlet Temperature is 355K:

Table 4.1 is obtained by using an engineering equation solver (EES). The thermodynamic values of the stage-I using R23 fluid when the first turbine inlet temperature (T_{11}) is 355K.

Table 4.1. Thermodynamic properties of R23 in the Stage-I

Point	State	Temperature (K)	Pressure (kPa)	Enthalpy (kJ/kg)	Entropy (kJ-kg/K)
11	Superheated vapor	355	1380	433.2	1.874
12	Superheated vapor (Scroll Turbine)	289.6	397.6	387.8	1.874
13	Superheated vapor	218.7	397.6	333.2	1.658
14	Saturated liquid	218.7	397.6	120	0.6825
15	Sub-cooled liquid (Pump)	219.1	1380	120.8	0.6825
16	Saturated liquid	252.7	1380	167.1	0.8789
17	Saturated vapor	252.7	1380	338.8	1.558

Table 4.2 shows the thermodynamic values of the stage-II using R23 fluid when the first turbine inlet temperature (T_{11}) is 355K.

Table 4.2. Thermodynamic properties of R23 in the Stage-II

Point	State	Temperature (K)	Pressure (kPa)	Enthalpy (kJ/kg)	Entropy (kJ-kg/K)
21	Superheated vapor	281.4	275	383	1.9
22	Superheated vapor (Scroll Turbine)	234.5	100	352.7	1.9
23	Superheated vapor	190.9	100	323.7	1.763
24	Saturated liquid	190.9	100	84.91	0.5118
25	Sub-cooled liquid (Pump)	191	275	98.17	0.5118
26	Saturated liquid	210.4	275	109.4	0.6331
27	Saturated vapor	210.4	275	330.7	1.686

Table 4.3 shows the power output and thermal efficiency values of different fluid pairs when the first turbine inlet temperature (T_{11}) is 355K. According to the results obtained, the highest power output was seen in the R23 + R23 pair as 18.84 kW and the highest thermal efficiency was obtained in the RC318 + RC318 pair as 6.708.

Table 4.3. System performance for different refrigerant pairs at 355K.

Working Fluids	**Turbine Inlet Temperature (K)**	**Power output (kW)**	**Thermal Efficiency (%)**
R134a + R134a	355	14.31	6.251
R410a + R410a	355	18.57	6.165
RC318 + RC318	355	8.097	**6.708**
R407C + R407C	355	16.24	6.057
R22 + R22	355	15.23	6.235
R23 + R23	355	**18.84**	6.484
R116 + R116	355	11.47	6.192
R218 + R218	355	8.64	6.083

For Turbine Inlet Temperature is 425K:

The thermodynamic values of the stage-I using R23 fluid when the first turbine inlet temperature (T_{11}) is 425K are given in Table 4.4.

Table 4.4. Thermodynamic properties of R23 in the Stage-I

Point	**State**	**Temperature (K)**	**Pressure (kPa)**	**Enthalpy (kJ/kg)**	**Entropy (kJ-kg/K)**
11	Superheated vapor	425	1380	496.4	2.037
12	Superheated vapor (Scroll Turbine)	355.6	397.6	440.1	2.037
13	Superheated vapor	218.7	397.6	333.2	1.658
14	Saturated liquid	218.7	397.6	120	0.6825
15	Sub-cooled liquid (Pump)	219.1	1380	120.8	0.6825
16	Saturated liquid	252.7	1380	167.1	0.8789
17	Saturated vapor	252.7	1380	338.8	1.558

Table 4.5 represents the thermodynamic values of the stage-II using R23 fluid when the first turbine inlet temperature (T_{11}) is 425K.

Table 4.5. Thermodynamic properties of R23 in the Stage-II.

Point	State	Temperature (K)	Pressure (kPa)	Enthalpy (kJ/kg)	Entropy (kJ-kg/K)
21	Superheated vapor	347.3	275	434.1	2.063
22	Superheated vapor (Scroll Turbine)	296.3	100	395.8	2.063
23	Superheated vapor	190.9	100	323.7	1.763
24	Saturated liquid	190.9	100	84.91	0.5118
25	Sub-cooled liquid (Pump)	191	275	101.5	0.5118
26	Saturated liquid	210.4	275	109.4	1.939
27	Saturated vapor	210.4	275	330.7	1.686

Table 4.6 shows the power output and thermal efficiency values of different fluid pairs when the first turbine inlet temperature (T_{11}) is 425K. According to the results obtained, the system's highest power output and thermal efficiency values were obtained when using R23 + R23 pair as the value of 23.82 kW and 6.818, respectively. This means as seen from table 8, R23 + R23 pair gives the highest power output and thermal efficiency when the input temperature of the turbine-I rises.

Table 4.6. System performance for different refrigerant pairs at 425K.

Working Fluids	**Turbine Inlet Temperature (K)**	**Power output (kW)**	**Thermal Efficiency (%)**
R134a + R134a	425	18.16	6.049
R410a + R410a	425	23.63	6.418
RC318 + RC318	425	9.994	5.338
R407C + R407C	425	20.65	6.13
R22 + R22	425	19.44	6.524
R23 + R23	425	**23.82**	**6.818**
R116 + R116	425	14.07	5.736
R218 + R218	425	10.64	5.176

Figure 4.4 indicates power output values at 355K, 390K and 425K turbine inlet temperature (T_{11}) values for each refrigerant pair. It is observed that the RC318 + RC318 pair gives the lower power output at each temperature value. On the other hand, the R23 + R23 pair gives the higher power output at each temperature. The lowest power output was obtained as 8.097 kW at 355 K turbine inlet temperature (T_{11}) when using the R318 pair, and the highest value determined as 23.82 kW at 425 K when using the R23 pair.

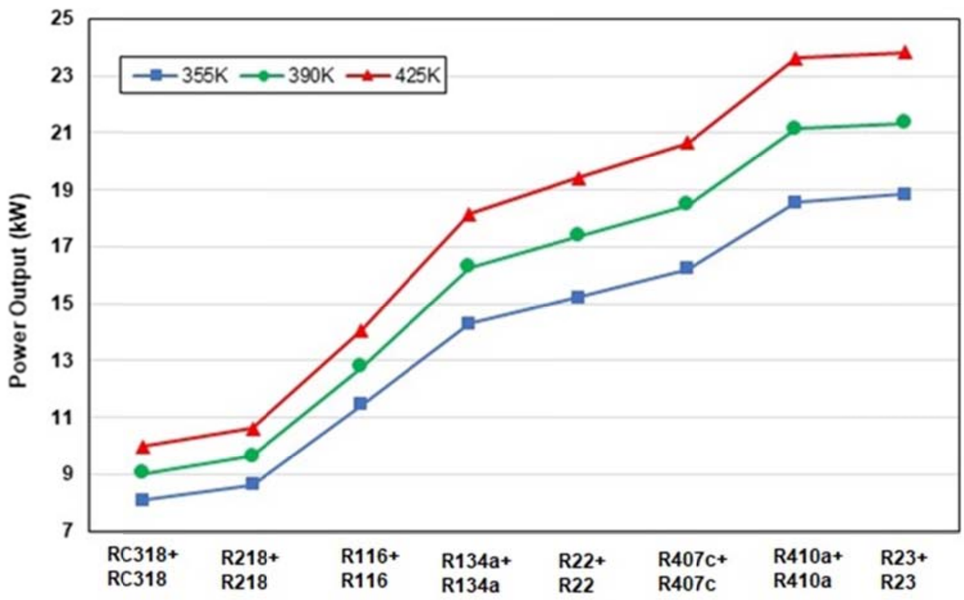

Figure 4.4. Power outputs when using different working fluid pairs at different temperatures

The relationship between refrigerant pairs for each temperature is presented in Figure 4.5. Increasing the turbine's inlet temperature has a negative impact on the thermal efficiency of the RC318 + RC318 pair. That thermal efficiency dramatically decreases from 6.708 to 5.338. It is observed that the thermal efficiency of R22, R407c, R410a and R23 increases as the temperature increases. On the other hand, in other refrigerants, the thermal efficiencies decreased as the temperature increased.

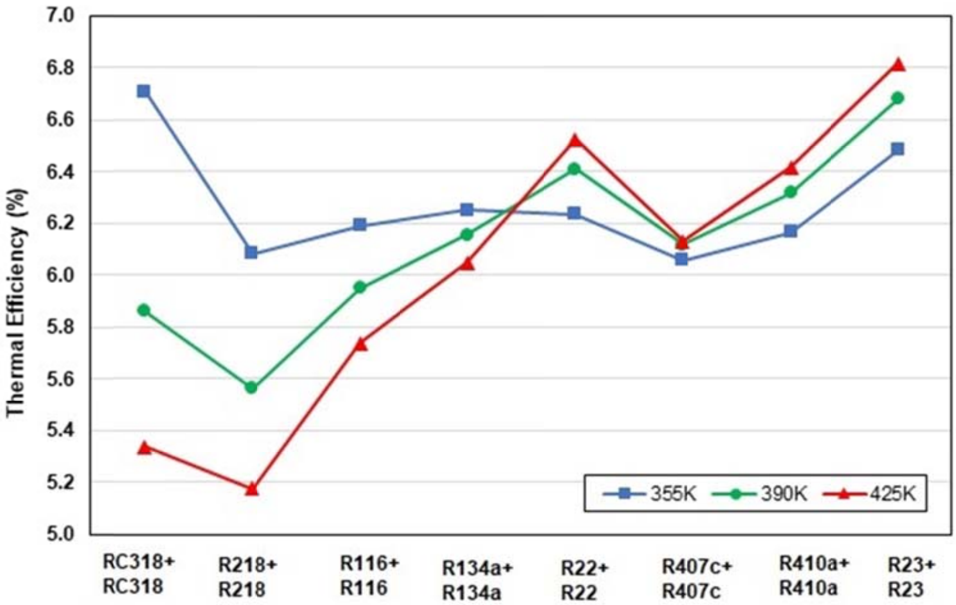

Figure 4.5. The system's thermal efficiency value for different working fluid pairs at the 355K, 390K and 425K.

Figure 4.6 shows power output from 8 different fluid pairs according to the turbine inlet temperature. It has been observed that the R410a + R410a pair gives about the same power output as the R23 + R23 pair, with a difference of about one percent at all temperatures. And between all of the pairs, the RC318 + RC318 pair gave the smallest net power output for each turbine inlet temperature (T_{11}) value.

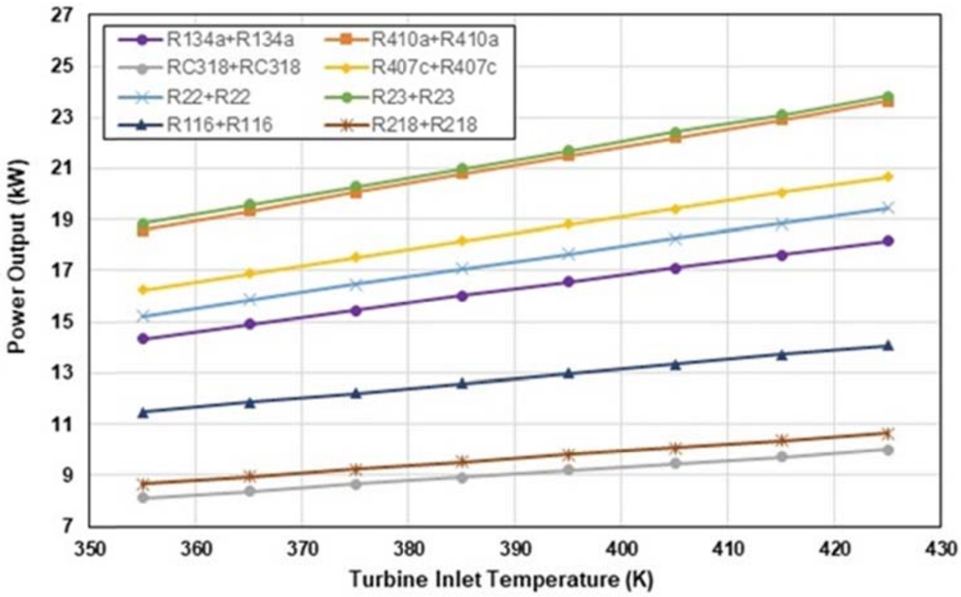

Figure 4.6. System net power output according to different pairs and temperatures.

Figure 4.7 presents thermal efficiency of the system versus turbine inlet temperature for R134a + R134a, R410a + R410a, RC318 + RC318, R407c + R407c, R22 + R22, R23 + R23, R116 + R116 and R218 + R218 refrigerant pairs. It is seen that when the R23 + R23 pair is used and turbine inlet temperature is 425 K in the ORC system, the thermal efficiency is 4.31% greater than the R22 + R22 pair. The system's thermal efficiency increases with temperature when R23 + R23, R22 + R22, R410a + R410a and R407c + R407c refrigerant pairs use. The thermal efficiency of other pairs decreases when the temperature is increased. On the other hand, when R218 + R218 pair is used, the smallest system thermal efficiency value among the other pairs was obtained at all temperatures.

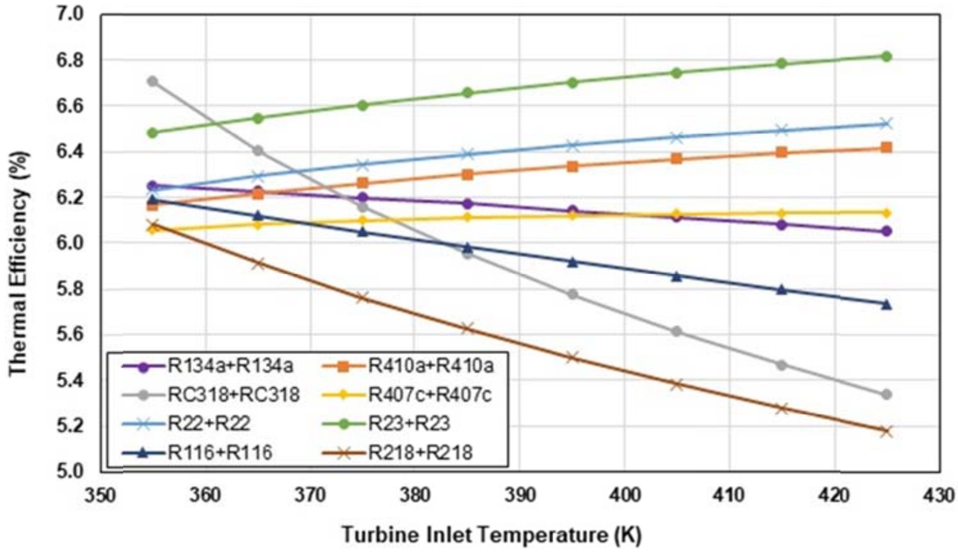

Figure 4.7. Thermal efficiency of the system versus turbine inlet temperature for different refrigerant pairs.

4.3. R245fa At Two Stage for Different Working Temperatures

With the EES (Engineering Equation Solver) software program thermodynamic properties of the R245fa refrigerant in the first and second stages were determined. EES simplifies the process. EES groups equations and automatically identifies that need to be solved and instead of assignments normally used in formal programming languages uses equations (Davidson, 1977). The effect on the system in the same situation is calculated by changing the evaporator inlet temperature (T_w).

For Evaporator Inlet Temperature is 400K:

Table 4.7 is shows the thermodynamic values of the first stage using R245fa fluid when the evaporator inlet temperature (T_w) is 400K.

Table 4.7. Thermodynamic properties of R245fa in the first stage

Point	**State**	**Temperature (K)**	**Pressure (kPa)**	**Enthalpy (kJ/kg)**	**Entropy (kJ-kg/K)**
11	Superheated vapor	418.5	1380	529.0	1.925
12	Superheated vapor (Scroll Turbine)	382	397.6	501.2	1.925
13	Superheated vapor	331.3	397.6	447.9	1.776
14	Saturated liquid	328	397.6	273.1	1.243
15	Sub-cooled liquid (Pump)	328.5	1380	273.9	1.243
16	Saturated liquid	377	1380	345.8	1.447
17	Saturated vapor	377	1380	476.3	1.793

Table 4.8 shows the thermodynamic values of the second stage using R245fa fluid when the evaporator inlet temperature (T_w) is 400K.

Table 4.9 shows the power output, thermal efficiency and exergy efficiency values of different evaporator inlet temperature (T_w) for R245fa refrigerant at both stages. According to the results, the highest power output, thermal efficiency and exergy efficiency values were obtained as 18.99 kW, 8.856% and 48.55%, respectively at 400K.

Table 4.8. Thermodynamic properties of R245fa in the second stage

Point	**State**	**Temperature (K)**	**Pressure (kPa)**	**Enthalpy (kJ/kg)**	**Entropy (kJ-kg/K)**
21	Superheated vapor	366.8	275	487.3	1.910
22	Superheated vapor (Scroll Turbine)	342.0	100	465.8	1.910
23	Superheated vapor	290.9	100	418.0	1.759
24	Saturated liquid	288.0	100	219.1	1.068
25	Sub-cooled liquid (Pump)	288.1	275	225.2	1.068
26	Saturated liquid	339.2	275	459.3	1.831
27	Saturated vapor	316.1	275	256.6	1.192

Table 4.9. System performance for different temperature for R245fa refrigerant.

Turbine Inlet Temperature (K)	**Power output (kW)**	**Thermal Efficiency (%)**	**Exergy Efficienfy System(%)**
400	**18.99**	**8.856**	**48.55**
405	18.22	8.274	44.06
410	17.73	7.846	40.63
415	17.40	7.513	37.87
420	17.19	7.246	35.59
425	17.06	7.025	33.66

For Evaporator Inlet Temperature is 425K:

Table 4.10 and 4.12 show the thermodynamic values of the first stage and second stage using R245fa fluid when the evaporator inlet temperature (T_w) is 425K, respectively.

Table 4.10. Thermodynamic properties of R245fa in the stage-I

Point	State	Temperature (K)	Pressure (kPa)	Enthalpy (kJ/kg)	Entropy (kJ-kg/K)
11	Superheated vapor	423.5	1380	535.1	1.940
12	Superheated vapor (Scroll Turbine)	387.2	397.6	506.7	1.940
13	Superheated vapor	331.3	397.6	447.9	1.776
14	Saturated liquid	328	397.6	273.1	1.243
15	Sub-cooled liquid (Pump)	328.5	1380	273.9	1.243
16	Saturated liquid	377	1380	345.8	1.447
17	Saturated vapor	377	1380	476.3	1.793

Table 4.11. Thermodynamic properties of R245fa in the stage-II

Point	State	Temperature (K)	Pressure (kPa)	Enthalpy (kJ/kg)	Entropy (kJ-kg/K)
21	Superheated vapor	372	275	492.6	1.924
22	Superheated vapor (Scroll Turbine)	347.2	100	470.8	1.924
23	Superheated vapor	290.9	100	418.0	1.759
24	Saturated liquid	288	100	219.1	1.068
25	Sub-cooled liquid (Pump)	288.1	275	224.8	1.068
26	Saturated liquid	344.4	275	464.5	1.846
27	Saturated vapor	316.1	275	256.6	1.192

Figure 4.8 shows thermal efficiency and power output relation between 400K and 425K evaporator inlet temperatures. As can be seen from the figure, there is an inverse proportion between thermal efficiency and power output with evaporator inlet temperature. For the system, both net electrical power and thermal efficiency decrease as ORC working temperature increases.

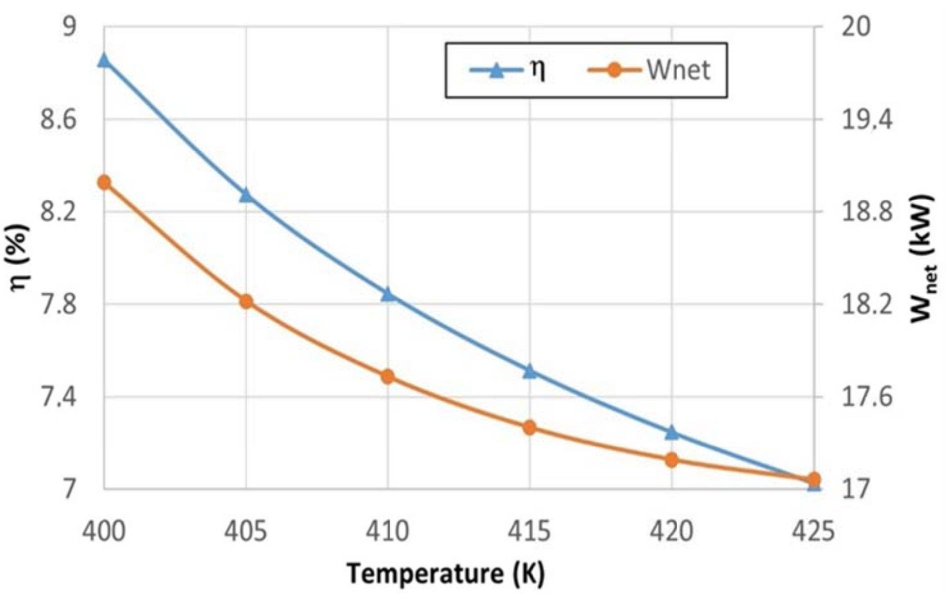

Figure 4.8. Thermal efficiency and power output values of the system versus evaporator inlet temperatures

The variation of the thermal and exergy efficiencies against the evaporator inlet temperature, for ORC system are shown in Figure 4.9. It is seen from the figure that, the exergy efficiency of the cycle decreases with increasing evaporator inlet temperature. At same time, thermal efficiency of the system decreases with increasing evaporator inlet temperature. The highest thermal and exergy efficiencies are seen at the 400K temperature.

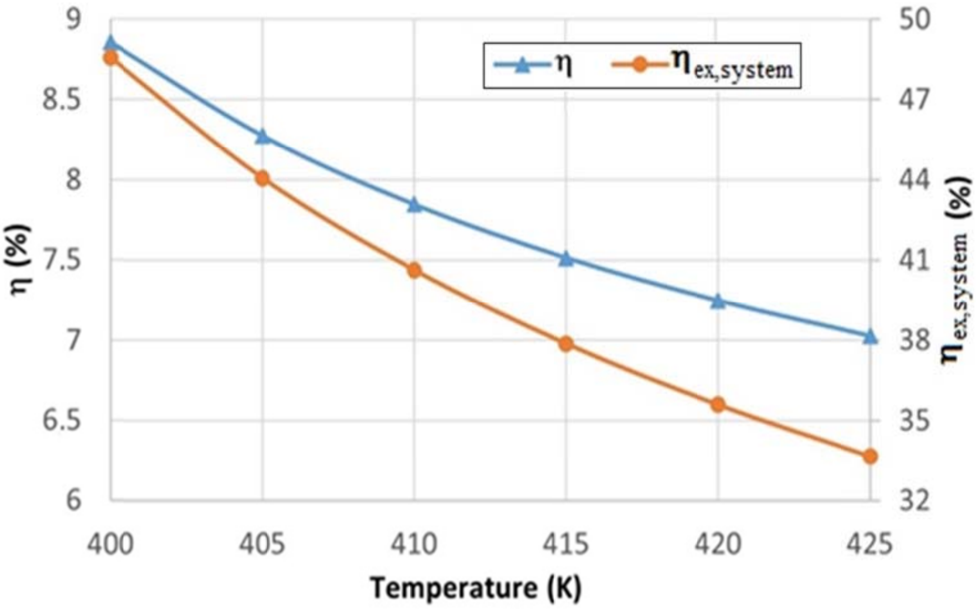

Figure 4.9. Thermal efficiency and exergy efficiency against evaporator inlet temperatures for the system.

Figure 4.10 represents exergy efficiency and exergy destruction values versus evaporator inlet temperature for Turbine1 and 2. It is seen from the figure that, exergy efficiency in the Turbine-1 decreases, while exergy destruction in the Turbine-1 increases with increasing evaporator inlet temperature. The smallest and highest exergy destructions in the Turbine-1 is 0.4514 kW and 0.6653 kW, respectively. The percentage of the exergy efficiency in Turbine-1 is 98.14 and 97.54 for 400K and 425K, respectively. Figure 4.10 also shows that, exergy efficiency in the Turbine-2 decreases, while exergy destruction in the turbine-2 increases, when evaporator inlet temperature is increased. The smallest and highest exergy destruction in the Turbine-2 is 0.1258 kW and 0.1496 kW, respectively. The percentage of the exergy efficiency in Turbine-2 is 99.25 and 98.48 for 400K and 425K, respectively.

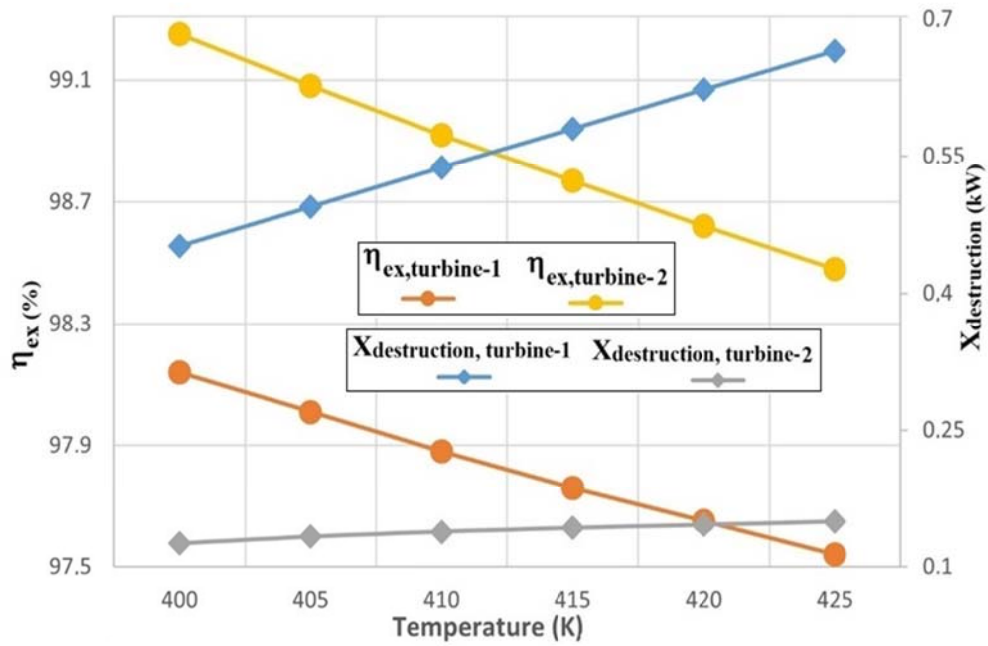

Figure 4.10. Exergy efficiency and exergy destruction values versus evaporator inlet temperature for Turbine1 and 2.

According to Figure 4.11 a and b, the exergy efficiency reduces with increasing evaporator inlet temperature of hot fluid for Pump1 and 2. In addition, the highest exergy efficiency is calculated as to be 6.18% and 83% for Pump-1 and 2, respectively when the evaporator inlet temperature is 400K. Exergy efficiency values decrease up to 5.48% and 44% for Pump1and 2.

The exergy destruction is increased from 11.2% to 12.6% for Pump1 and from 1.6% to 3.1% for Pump2 in figure 4.11 a and b. According to the results of calculations, it is seen from Figure 4.11 a and b; the highest exergy destruction is observed at the Turbine1 and 2 against to the smallest exergy efficiency is seen at the Condenser1 and 2 for 425K temperature.

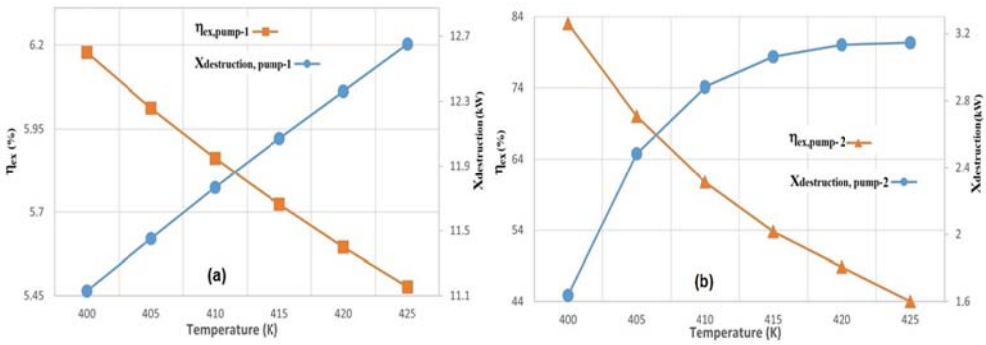

Figure 4.11. Exergy destruction and Thermal efficiency values when using R245fa at different evaporator inlet temperatures for (a) Pump1 and (b) Pump2.

Exergy efficiency values of ORC system components at 425K evaporator inlet temperature are shown in Figure 4.12. The greatest efficiencies were obtained in Turbine1 and 2 and in the Evaporator. Smallest efficiencies were obtained in both Condensers and in Pump1.

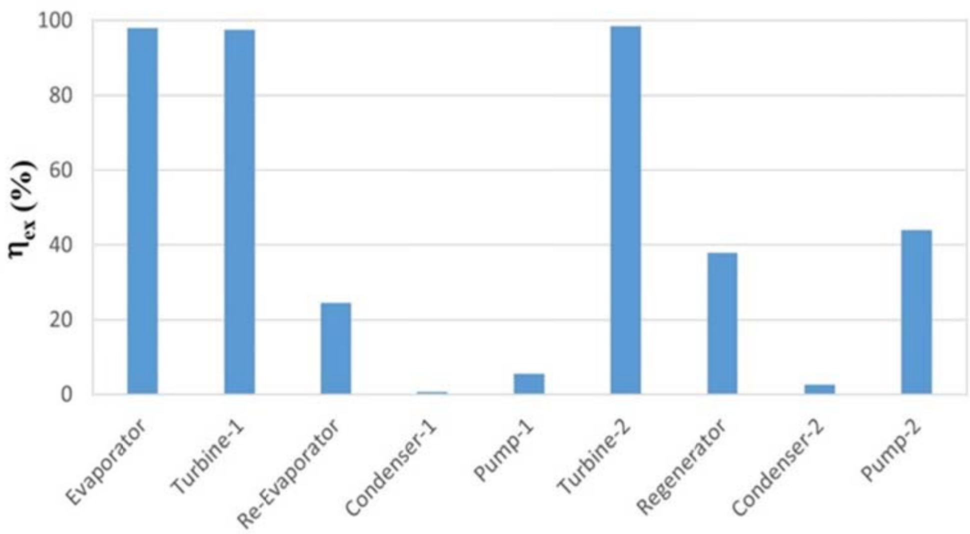

Figure 4.12. Exergy efficiency values of all components of the system at 425K evaporator inlet temperature

Exergy destruction of the turbines and pumps due to evaporator inlet temperature changes is given in Figure 4.13. The maximum exergy destruction is found in Pump1 compared to other components for all temperatures. Minimum exergy destruction is found in Turbine2 compared to other components for all temperatures.

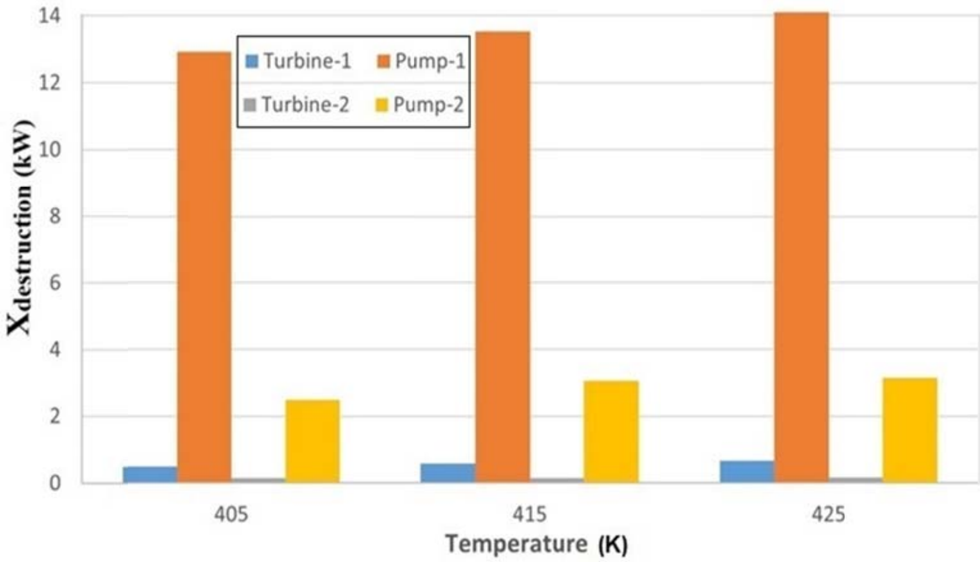

Figure 4.13. Exergy destruction at turbines and pumps for 405K, 415K and 425K.

Figure 4.14 shows that condenser 1 and 2 outlet temperature values for different refrigerants which is working at 405K. R23 + R23 couples gives smallest condenser 1 and 2 output temperatures which is 218.7K and 190.9K respectively. At the same working condition R245fa + R245fa couples givest highest condenser 1 and 2 output temperatures which is 328K and 288K respectively.

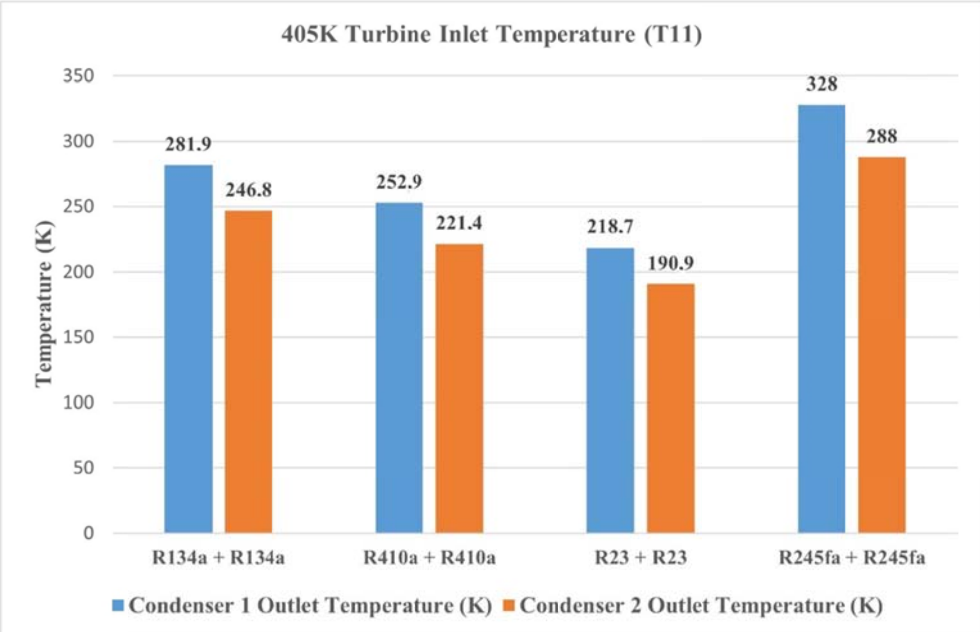

Figure 4.14. Condenser 1 and 2 outlet temperature values for different refrigerants at 405K.

5. CONCLUSION

First part of the thesis, thermodynamic analysis of a two stage organic Rankine cycle which is heated with solar collector is solved using EES program. The results can be summarized as follows:

- Highest thermal efficiency is observed at R227ea + R410a couple at 355K and 435K but the thermal efficiency of the system decreases when the temperature is increased. Also, net power output is lower than other couples.
- R290 + R410a couple gives highest net power output at 355K and 435K. But, R290 refrigerant belongs to A3 (higher flammability) group according to ASHRAE 34 Refrigerant Safety Classification. And this makes the system more dangerous.
- R134a + R410a couples' thermal efficiency is decreasing when temperature is increased. R32 + R410a couple gives %41 more power output then R134a + R410a.

Second part for the thesis, double stage organic Rankine cycle (ORC) which is heated with the solar collector is solved with the EES program. The results can be summarized as follows:

- Different solar collector temperatures are considered in the present analysis, the highest thermal efficiency and power output are achieved at 425K.
- The thermal efficiency values of the system at 325K turbine inlet temperature are observed as the highest value for the RC318 + RC318 pair. But that thermal efficiency value dramatically decreases when the solar collector temperature is increased.

- Among all refrigerants, R23 can be recommended for all working temperatures. Because R23 + R23 pair gives the highest net power output and thermal efficiency values for all temperatures and working fluids.
- As the turbine inlet temperature increases, the net power output of the system increases for all refrigerant pairs, but the system's thermal efficiency against turbine inlet temperature increases only when R23, R22, R410a and R407c refrigerant pairs are used.

Last part of the thesis, exergy analysis of a double stage organic rankine cycle using renewable energy. This work represents a comprehensive assessment of exergy analysis of the double stage ORC system. The Engineering Equation Solver is used to carry out various calculation of present analysis. In this work, the exergy destruction and exergy efficiency values of various components are obtained and compared. The results can be summarized as follows:

- The exergy destruction in Pump-1 is found higher than other components at all evaporator inlet temperature. As a result, at 425K, 14.11kW exergy destruction is obtained. The smallest exergy destruction is observed in Turbine-2. The exergy destruction in turbine-2 is found to be 0.133kW at 400K temperature.
- The highest exergy efficiency is observed at the Turbine-2 as 98.48%. The minimum exergy efficiency is seen at the Condenser-1 for 425K temperature as 0.7%.
- The highest thermal and exergy efficiencies of the whole system were obtained at 400K temperature as 8.85% and 48.55%, respectively. The exergy efficiency of the cycle decreases with increase in evaporator inlet temperature. At same time, thermal efficiency of the system decreases with increase in evaporator inlet temperature.

- Accourding to ORC which is working at the atmosphere condition is R245fa + R245fa couples suitable because of that couples givest highest condenser 1 and 2 output temperatures which is 328K and 288K respectively.

5.1. Future Works

Since a costing analysis should be performed to estimate the initial capital costs, operating and maintenance costs, and total costs for each component in the system are required in $/h, it is designed to perform an exergoeconomic analysis with data obtained from a real operating conditions for a double stage ORC system in future stages of the study. Furthermore, further research into the costs associated with components of the organic Raknine cycle system, as well as further investigation into exergy fuel input costs, will be more beneficial, especially when considering solar thermal sources, as in this study, and will improve the accuracy of the exergoeconomic analysis.

REFERENCES

Obafunmi, Jaiyejeje S., 2014. Thermodynamic Analysis of Organic Rankine Cycles, Eastern Mediterranean University Gazimağusa, North Cyprus.

Quoilin, S., Orsz, M., Hemond., Lemort, V., 2011, Performance and design optimization of a low-cost solar organic Rankine cycle for remote power generation, Solar Energy 85 (2011) 955–966.

G. Becquin, M. Lehar, Two algorithms for reliable estimation of organic Rankine performance, J. Eng. Gas Turbines Power 13 (2012) 4044504-1e 4044504-5.

E. Wali, "Optimum working fluids for solar powered Rankine cycle cooling of buildings," Solar Energy, vol. 25, pp. 235–241, 1980.

Davidson, T.A.,1977, Design and Analysis of a 1 kW Rankine Power Cycle, Employing a Multi-Vane Expander, for Use with a Low Temperature Solar Collector. Master's Thesis, Massachusetts Institute of Technology, Cambridge, MA, USA.

Chen, H., Goswami, D.Y., Stefanakos, E.K., A review of thermodynamic cycles and working fluids for the conversion of low-grade heat. Renew Sustain Energy Rev 2010;14:3059–67.

D. H. Lee, Organic rankine cycle power generator, 8th Fluid Machinery Core Technology Lecture of Korea Society for Fluid Machinery (2014) 169-179.

Eyidogan M, Kilic FC, Kaya D, Coban V, Cagman S (2016) Investigation of Organic Rankine Cycle (ORC) technologies in Turkey from the technical and economic point of view. Renewable and Sustainable Energy Reviews; 58:885-895.

Joshi A.S., Dincer I., Reddy B.V. Solar hydrogen production: a comparative performance assessment. International Journal of Hydrogen Energy 2011;36(17):11246e57.

Lim, H.S., Choi, B.S., Park, M.R., Hwang, S.C., Park, J.Y., Seo, J., Bang, J.S., Kim, B.O., 2017. Performance evaluation of two-stage turbine for the organic rankine cycle system, Journal of Mechanical Science and Technology 31 (12) 5849~5855.

Wang, Q., Wang, J., Li, T., Meng, N., 2020. Techno-economic performance of two-stage series evaporation organic Rankine cycle with dual-level heat sources, Applied Thermal Engineering 171 (2020) 115078.

Bertrand, F. T., Papadakis, G., Lambrinos, G., Frangoudakis, A,. 2009. Fluid selection for a low temperature solar organic Rankine cycle. Applied Thermal Engineering 29 2468–2476.

B.F. Tchanche, G. Papadakis, G. Lambrinos, A. Frangoudakis, Criteria for working fluids selection in low-temperature solar organic Rankine cycles, in: Proc. Eurosun Conf., Lisbon, Portugal, 7–10 October, 2008.

V. Maizza, A. Maizza, Working fluids in non-steady flows for waste energyrecovery systems, Applied Thermal Energy 16 (7) (1996) 579–590.

A. Borsukiewcz-Gozdur, W. Nowak, Comparative analysis of natural and synthetic refrigerants in application to low temperature Clausius–Rankinecycle, Energy 32 (2007) 344–352.

Drescher U, Bruggemann D., Fluid selection for the organic Rankine cycle (ORC) in biomass power and heat plants. Applied Thermal Engineering 2007, 27:2238.

Saleh B, Koglbauer G, Wedland M, Fischer J. Working fluids for low-temperature organic Rankine cycles. Energy 2007 (32) 1210e21.

Dincer I, Rosen MA. Thermodynamic aspects of renewables and sustainable development. Renewable and Sustainable Energy Reviews 2005; 9:169–189.

Wang X. D. Zhao L. Wang J.L, Zhang W. Z. , Zhao X .Z., W. Wu. 2009. Performance evaluation of low-temperature Solar Rankine cycle system utilizing R245fa. Solar Energy84 (2010), 353-364.

Dincer I, Rosen MA. Exergy: energy, environment and sustainable development. NY: Elsevier; 2007.

Wang L, Yang Y, Morosuk T, Tsatsaronis G. Advanced thermodynamic analysis and evaluation of a supercritical power plant. Energies 2012;5:1850–63.

O. Kaska, "Energy and exergy analysis of an organic Rankine for power generation from waste heat recovery in steel industry," Energy Conversion and Management, vol. 77, pp. 108-117, 2014.

Tsatsaronis G, Park M. On avoidable and unavoidable exergy destructions and investment costs in thermal systems. Energy Convers Manage 2002;43:1259–70.

Cengel, Yunus A., Boles MA (2010) Thermodynamics: an engineering approach, 7th edn. McGrawHill, New York.

El-Emam RS, Dincer I. Exergy and exergoeconomic analyses and optimization of geothermal organic Rankine cycle. Appl Therm Eng 2013;59(1–2): 435–44.

Madhawa Hettiarachchi HD, Golubovic M, Worek WM, Ikegami Y. Optimum design criteria for an Organic Rankine cycle using low-temperature geothermal heat sources. Energy 2007;32:1698–706.

X. Wang, Y. Dai, Exergoeconomic analysis of utilizing the transcritical CO2 cycle and the ORC for a recompression supercritical CO2 cycle waste heat recovery: a Comparative study, Appl. Energy 170 (2016) 193e207.

Wall, G. (1998), “Exergetics”, Exergy Ecology Democracy, Sweden.

Rivero, R. ve Anaya, A. (1997), “Exergy Analysis of Industrial Processes: Energy-Economy-Ecology”, Latin American Applied Research, 27:191-205.

Kotas, T.J. (1995), “The Exergy Method of Thermal Plant Analysis”, Kriger Publising Comp, USA.

Çengel, Yunus A., Boles, M.A. (1998), “Thermodynamics, An Engineering Approach”, Mc. Graw Hill, USA.

Cengel, Yunus A., Dincer I., Energy, Entropy and Exergy Concepts and Their Roles in Thermal Engineering, Entropy (2001), 3, 116-149.

Bertrant, T.F., Papadakis, G., Lambrinos, G., Frangoudakis, A., 2008. Criteria for working fluids selection in low-temperature solar organic Rankine cycles. 1st International Congress on Heating, Cooling and Buildings.

Badr, O., Probert, S.D., and O'Callaghan, P.W., Selecting a working fluid for a Rankine-cycle engine, Applied Energy 21 (1985) 1-42.

Cengel, Yunus A., Boles, Michael A., Thermodynamics An Engineering Approach, 5th edition 554-555.

Li, X., Liu, T., Chen, L., 2018. Thermodynamic Performance Analysis of an Improved Two-Stage Organic Rankine Cycle, School of Mechanical Engineering, Tianjin Polytechnic University, Tianjin 300387, China.

Cengel, Yunus A., Heat Transfer, 2th edition 690-694.

Klein, S. A. (2003). Engineering Equation Solver - Manual. F-Chart Software, Box.

Aljundi, I.H., 2009. Energy and exergy analysis of a steam power plant in Jordan. Appl. Therm. Eng. 29, 324–328.

Kaushik, S. C., V. S. Reddy, and S. K. Tyagi. 2011. 'Energy and exergy analyses of thermal power plants a review. Renewable and Sustainable Energy Reviews 15 (4):1857–72.

Tsatsaronis, G., (1999), "Design Optimization Using Exergoconomics", Thermodynamic Optimization Of Complex Energy Systems, Nato Sciences, 3. High Technology, Volume 69.)

Bejan A, Tsatsaronis G, Moran M. Thermal design and optimization. New York: John Wiley and Sons Inc.; 1996.);

Klein, S. A. (2003). Engineering Equation Solver - Manual. F-Chart Software, Box.

CURRICULUM VITAE

Ahmet KAPLAN, enrolled in Mechanical Engineering Department of Çukurova University in Adana in 2013. He graduated from the department of Mechanical Engineering in 2017. Began his Master of Science in 2018. After completing his undergraduate studies he worked as a mechanical engineer at the Adana provincial directorate of national education in 2017. He is currently working as a mechanical engineer in the same department.